

# Recent Developments and Practical Feasibility of Polymer-Based Antifouling Coatings

Anna M. C. Maan, Anton H. Hofman, Wiebe M. de Vos,\* and Marleen Kamperman\*

While nature has optimized its antifouling strategies over millions of years, synthetic antifouling coatings have not yet reached technological maturity. For an antifouling coating to become technically feasible, it should fulfill many requirements: high effectiveness, long-term stability, durability, ecofriendliness, large-scale applicability, and more. It is therefore not surprising that the search for the perfect antifouling coating has been going on for decades. With the discovery of metal-based antifouling paints in the 1970s, fouling was thought to be a problem of the past, yet its untargeted toxicity led to serious ecological concern, and its use became prohibited. As a response, research shifted focus toward a biocompatible alternative: polymer-based antifouling coatings. This has resulted in numerous advanced and innovative antifouling strategies, including fouling-resistant, fouling-release, and fouling-degrading coatings. Here, these novel and exciting discoveries are highlighted while simultaneously assessing their antifouling performance and practical feasibility.

## 1. Introduction


Fouling, i.e., unwanted adhesion, is a complex and undesirable process where material from the environment, such as macromolecules, microorganisms, or suspended particles, adhere reversibly or irreversibly to a surface.<sup>[1]</sup> This process is a widespread obstacle, causing problems in medical, marine, and industrial applications. In medical applications, fouling poses significant health risks, including the spread of infectious diseases, implant rejection, and malfunction of biosensors. Industrial fouling occurs, for instance, in power plants, water-treatment systems and the food industry. It causes increased

energy needs, pipe blockage, reduced efficiency, and water contamination. In marine environments, ship hull biofouling increases drag, corrosion, fuel consumption and engine stress.<sup>[2]</sup> Effective fouling protection could save the global maritime industry alone an estimated 150 billion dollars annually.<sup>[3]</sup> Hence, there is a universal need to find ways to combat or minimize fouling. In fact, the search for effective antifouling technologies to combat fouling has been going on for centuries, and it has been undergoing extensive changes. Early generation antifouling systems were designed to be antimicrobial, which involved biocidal materials that could kill fouling organisms and consequently prevent their settlement. The developed antimicrobial systems varied from simple lead and copper sheets on wooden boats, to antimicrobial coatings containing copper,

arsenic, and mercury on ship hulls. Copper was an effective and widely used biocide, but only proved to be effective for a period of up to two years. When incorporating biocidal tributyltin (TBT) into existing coatings, this limited lifespan could be extended to more than 5 years. Unfortunately, the widespread use of these (heavy) metal-based antifouling coatings resulted in high-level contamination, and a global ban on their usage followed. Increased awareness of the negative environmental impact when using toxic biocides stimulated development of nontoxic, ecofriendly alternatives, including fouling-release coatings that incorporated polymers (e.g., silicones, fluoropolymers), waxes, or oils, and “natural” coatings that incorporated antifouling compounds extracted from organisms. Such natural coatings, however, were difficult to commercialize, due to the limited supply, high cost, short-term efficacy, and specificity of natural antifouling compounds. Moreover, despite their natural origin, these coatings still struggled to meet the environmental legislation requirements.<sup>[4–6]</sup> Instead, focus shifted toward polymer-based coatings, as they overcome many drawbacks of conventional coatings. Polymer-based coatings are cheap, nontoxic, biocompatible, easy to process, have a wide-range efficacy, and are highly versatile. Their functionalities and architectures can be easily modified, which allows tuning of interfacial properties and thereby the antifouling properties. More specifically, polymer brushes are well-known for their ability to transform the nature of a surface by creating a layer of just a few nanometers thick.<sup>[4,7,8]</sup> They are defined as a densely packed array of polymer chains, end-attached to an interface and stretched out into solution.<sup>[9–12]</sup> These brushes can act as a physical barrier

A. M. C. Maan, Dr. A. H. Hofman, Prof. M. Kamperman  
Polymer Science, Zernike Institute for Advanced Materials  
University of Groningen  
Nijenborgh 4, Groningen 9747 AG, The Netherlands  
E-mail: marleen.kamperman@rug.nl

Prof. W. M. de Vos  
Membrane Science and Technology, MESA+ Institute for Nanotechnology  
University of Twente  
P.O. Box 217, Enschede 7500 AE, The Netherlands  
E-mail: w.m.devos@utwente.nl

 The ORCID identification number(s) for the author(s) of this article can be found under <https://doi.org/10.1002/adfm.202000936>.

© 2020 The Authors. Published by WILEY-VCH Verlag GmbH & Co. KGaA, Weinheim. This is an open access article under the terms of the Creative Commons Attribution License, which permits use, distribution and reproduction in any medium, provided the original work is properly cited.

DOI: 10.1002/adfm.202000936

between the surface and approaching foulants, in two ways: 1) If a foulant would approach the surface, the resulting compression of the polymer chains would reduce the total number of possible conformations, which is entropically unfavorable, subsequently causing steric repulsion and preventing adsorption. 2) In case of a tightly bound hydration layer surrounding the brushes, water would have to be removed to make place for an adhering fouling particle. Such a dehydration process is thermodynamically unfavorable, leading to repulsion of approaching foulants.<sup>[1,13–15]</sup>

These are the main reasons why research into polymer-based antifouling coatings has blossomed over the last couple of years, and thus explains why our focus lies on reviewing these particular types of coatings.

Still, achieving an efficient way of fouling control remains a major challenge in many applications, caused by the poor mechanical stability and/or short-term antifouling durability of existing antifouling coatings. The latter is partly related to the large variety of foulants present within the system of interest. The major types of fouling can be categorized as follows:

- i. Organic fouling: accumulation of organic material, like macromolecules (proteins, polysaccharides, carbohydrates, lipids, etc.).
- ii. Inorganic fouling: precipitation of inorganic material, such as salts and metal oxides, often the result of crystallization or corrosion processes.
- iii. Particulate fouling: accumulation of particles (e.g., colloidal particles)
- iv. Biological fouling (“biofouling”): settlement and accumulation of biological matter, resulting in conditioning films (macromolecules), which can grow into biofilms (microorganisms) and lead to macroscopic biofouling (macroorganisms).<sup>[2,16,17]</sup>

Fouling can also involve more than one foulant or fouling mechanism, and is then referred to as composite fouling.<sup>[16]</sup>

Since fouling mainly depends on surface properties, such as the surface energy, wettability, and microtexture, modifying the surface structure provides a straightforward method of fouling control. The most common and successful method to reach this goal is by treating the substrate with an antifouling coating. The existence of different types of fouling demands a variety of antifouling coating strategies, including fouling-resistant, fouling-release and fouling-degrading coatings (**Figure 1**).

- i. Fouling-resistant: prevents adhesion of proteins, algae, and/or bacteria, often attributed to the formation of a strongly hydrated surface, as this provides a physical and free energy barrier to foulants.<sup>[1,18–20]</sup>
- ii. Fouling-release: allows weak foulant-surface adhesion, but simultaneously facilitates easy removal of adsorbed foulants by the application of a limited shear or mechanical force (e.g., via a water jet, or an external trigger).<sup>[1,18–20]</sup>
- iii. Fouling-degrading: degrades adsorbed organic material via oxidizing agents and/or kills (attached) bacteria and other microorganisms by the action of bactericidal functionalities.<sup>[19,20]</sup>

Several means have been developed to realize these three antifouling strategies, including modification of the surface chemistry, surface topography, and architecture (**Figure 2**).



**Anna M. C. Maan** received her M.Sc. in chemistry from the University of Groningen, The Netherlands, in 2018. She is currently pursuing a Ph.D. in polymer chemistry from the Polymer Science Group at the University of Groningen, under the supervision of Prof. Marleen Kamperman and Prof. Wiebe M. de Vos. Her research

focuses on the development of easily applicable and reversible antifouling coatings.



**Anton H. Hofman** received his Ph.D. degree in 2016 from the University of Groningen on the topic of hierarchically self-assembling comb-shaped copolymers. He subsequently joined the Physical Chemistry and Soft Matter Department at Wageningen University as a postdoctoral researcher where he designed hydrophobic/strong polyelectrolyte diblock copolymers for use

in enhanced underwater adhesives. In 2019, he returned to Groningen to work as a research fellow in the newly established Polymer Science Group. His research interests include the synthesis of complex macromolecular materials, block copolymer self-assembly, and supramolecular chemistry.



**Wiebe M. de Vos** received his Ph.D. in 2009 from Wageningen University on the topic of polymer brushes and subsequently moved to Bristol University, where he studied the structure of polymeric surface coatings under confinement. In 2012, he moved to the University of Twente, where he leads the research group “Membrane

Surface Science” (MSuS). Here, he combines his background in the fundamentals of surface science with the much more applied field of membranes. He develops advanced polymeric coatings to create multifunctional and highly selective membranes. He became an associate professor in 2016 and an adjunct professor in 2019.

The first two approaches emphasize the change in surface characteristics by applying a coating, while the role of the coating interior is included in the latter.

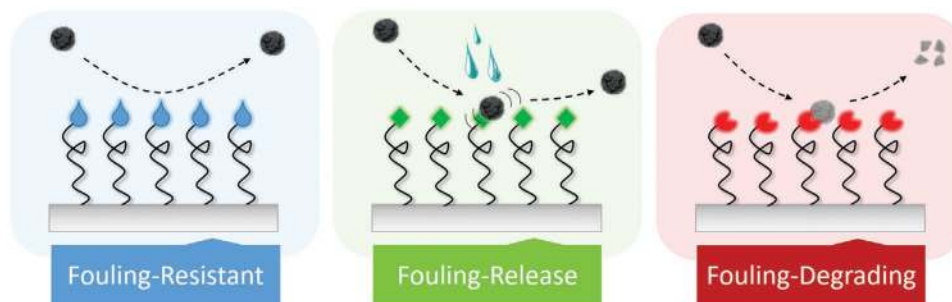


**Figure 1.** Schematic illustration of the three principal antifouling strategies: 1) preventing foulants from attaching to the surface (fouling-resistant), 2) weakening the interaction between foulant and surface (fouling-release), and 3) degrading/killing biofoulants (fouling-degrading).

Surface chemistry influences the way foulants interact with the surface. According to the rules outlined by Whitesides and co-workers, surfaces resisting fouling have three common features: they are hydrophilic, hydrogen bond-forming and electrically neutral.<sup>[21]</sup> Indeed, multiple studies found that the antifouling ability of hydrophilic and zwitterionic surfaces is related to the high hydration and surface energy, because the tightly bound water layer forms a physical and free energy barrier, preventing adsorption.<sup>[22]</sup> On the other hand, a lower surface energy, such as a hydrophobic surface, provides the surface with a higher self-cleaning potential. In addition to the surface energy, surface charge can also play an important role in preventing nonspecific adhesion. Moreover, by incorporating (charged) antimicrobial/biocidal moieties inside the coating, microorganisms can be killed upon settlement. Hence, by manipulating the surface chemistry, one can either develop fouling-resistant, fouling-release, or fouling-degrading coatings.<sup>[18]</sup>

Surface topography can impede the settlement of microorganisms by imposing size restrictions. Microorganisms prefer to settle in areas that are slightly larger than themselves in order to achieve maximum protection and surface area contact. Hence, developing a micro- or nanostructure on top of the surface of interest can restrict the number of attachment possibilities, thereby limiting foulant adhesion and facilitating easy removal of foulants in case of settlement. This antifouling approach therefore enables the development of both fouling-resistant and fouling-release (self-cleaning) coatings.<sup>[2]</sup>

In contrast to surface topography, which minimizes fouling by modification of the micro- or nanostructure of the coating surface, the architecture involves structuring of the coating interior. This strategy is most relevant when working with structured soft matter, such as polymer brushes. In case of a polymer brush, foulants can adhere in three ways: penetrate

through and adsorb onto the substrate (primary adsorption), adsorb on top of the brush (secondary adsorption) or adsorb inside the brush (tertiary adsorption).<sup>[23]</sup> Tuning of the brush architecture (i.e., linear brush, bottlebrush, cyclic brush, etc.) may enhance control over the surface formation and coverage, provide better access to specific functional groups, enable the formation of structured surfaces, and limit the interaction between foulants and the underlying surface.<sup>[7,8]</sup> The grafting density, thickness and flexibility of the polymer brush are essential parameters that should always be taken into account when designing such coatings.<sup>[24]</sup>

Over the last two decades, considerable effort has been devoted to the design and construction of antifouling coatings. Fouling-degrading coatings evolved from (in)soluble matrix coatings and self-polishing copolymer coatings (e.g., organotin paints) to cationic coatings (quaternary ammonium compounds, metallic composites) and enzyme-based coatings. Fouling-release coatings were predominantly constructed from hydrophobic materials (silicones, fluorine-based) or by patterning surfaces (“Sharklet”). Fouling-resistant coatings were mostly based on poly(ethylene glycol) and other hydrophilic polymers (polyacrylates, polysaccharides), although the interest in these materials recently shifted toward zwitterionic polymers.<sup>[3,25,26]</sup> For an overview of the broad range of antifouling materials and films, we refer to some extensive reviews that have been written previously.<sup>[3,23,25,27]</sup> This work is not intended as a comprehensive overview of all possible strategies to obtain an antifouling coating, but rather aims at highlighting novel and exciting discoveries that were found over the past five years. Apart from discussing natural and synthetic antifouling strategies (Sections 2-5), we would like to emphasize the superior antifouling potential when combining several strategies into a single synergistic coating (Section 6). While discussing the many interesting lab-designed antifouling coatings,

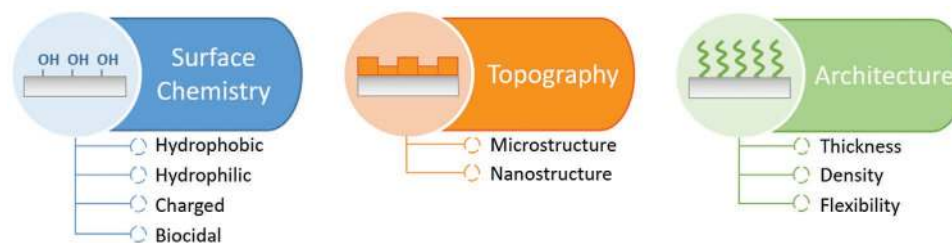


**Figure 2.** Three approaches to endow a surface with antifouling properties: 1) modification of surface chemistry, 2) surface topography, and 3) the coating architecture.



it is important to maintain a critical mindset concerning their long-term stability and large-scale applicability, which will therefore be the focus of the final section (Section 7).

## 2. From Natural to Biomimetic Coatings

When designing antifouling coatings, it is essential to derive inspiration from biological systems. Owing to the complexity of fouling, nature has developed clever combinations of physical and chemical strategies to minimize nonspecific adhesion, including chemical secretions, microtextures, and self-cleaning methods.<sup>[2,28]</sup> For example, the endothelium, the inner surface of our blood vessels, includes a combination of these methods to resist fouling. Its cobblestone-like morphology, together with a layer of negatively charged glycoproteins, prevents any platelet or leukocyte from attaching (Figure 3).<sup>[1,29,30]</sup> Inspired by these natural systems, researchers have developed new and effective antifouling strategies that are more sustainable and ecofriendly than conventional strategies, such as the toxic metal-leaching paints.<sup>[2]</sup> Bioinspiration has resulted in two main strategies for antifouling surface modification, namely physical altering of surface microtopography and chemical surface modification.<sup>[19,31]</sup>

### 2.1. Microtopography

Surfaces with complex topographies, such as those mimicking the skin of sharks or the surface of lotus leaves, often possess

excellent biofouling inhibition and/or self-cleaning properties.<sup>[3]</sup> Several mechanisms could be at play: superhydrophobicity, capillary forces, attachment point minimization, and drag reduction. A microstructured surface consists of an array of small features, in between which air may get trapped, resulting in a superhydrophobic surface.<sup>[19]</sup> Conversely, when in water, the capillary forces present in such small nanostructures may bind water so strongly that it cannot be replaced through the adhesion of foulants, thereby preventing them from firm bonding.<sup>[32]</sup> Moreover, microorganisms respond to topographies that are similar to their body size, in order to gain shelter from shear stress and/or predation, and to maximize their surface contact area. By creating surfaces with textures smaller than the microorganism body size, the number of attachment points can be minimized, and microorganisms are discouraged from adhering.<sup>[32,33]</sup> Additionally, in the specific case of sharks, the riblet micropattern on their scales reduces drag, which allows the water layer next to the skin to move faster, thereby reducing and removing settled microorganisms.<sup>[2]</sup> The size of the surface patterns (i.e., length, height and width of micro- or nanostructures), their distribution (i.e., random or ordered) as well as the shape of the motifs can all dramatically affect the final surface behavior.<sup>[4,34]</sup> This section presents a wide variety of structured antifouling surfaces developed and optimized by nature, which nowadays function as an inspirational source for the development of new synthetic antifouling coatings. For a thorough description of the relationship between natural hierarchical structures and their antifouling performance, we would like to refer to other publications.<sup>[1,33,35]</sup>

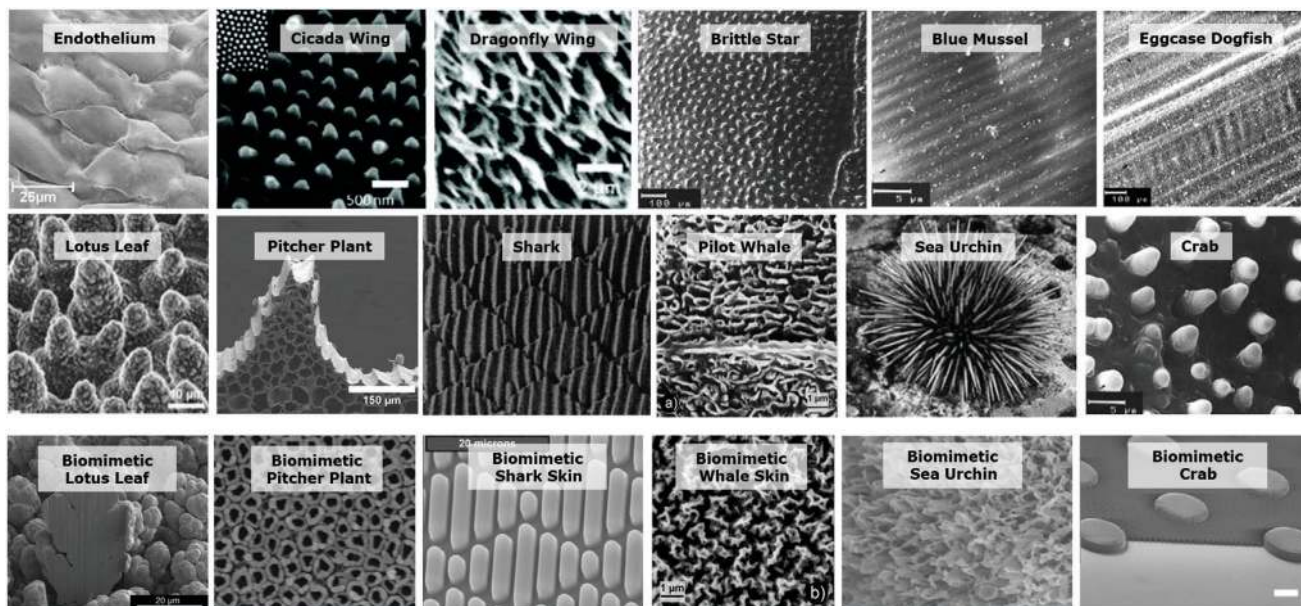


**Figure 3.** SEM images of natural and biomimetic microtextured surfaces. The third row shows artificial structured surfaces inspired by the microtopographies of the row above. Endothelium is adapted with permission.<sup>[36]</sup> Copyright 2010, Wiley-VCH. Cicada wing and dragonfly wing are adapted with permission.<sup>[37]</sup> Copyright 2016, The Royal Society of Chemistry. Brittle star, blue mussel, eggcase dogfish, and crab are adapted with permission.<sup>[33]</sup> Copyright 2004, Taylor & Francis. Lotus leaf is adapted with permission.<sup>[19]</sup> Copyright 2016, Springer Nature. Pitcher plant is adapted with permission.<sup>[38]</sup> Copyright 2015, Springer Nature. Shark is adapted with permission.<sup>[39]</sup> Copyright 2000, Springer-Verlag. (Biomimetic) whale skin is adapted with permission.<sup>[32]</sup> Copyright 2010, Wiley-VCH. (Biomimetic) sea urchin is adapted with permission.<sup>[40]</sup> Copyright 2018, Elsevier. Biomimetic lotus leaf is adapted with permission.<sup>[41]</sup> Copyright 2014, American Chemical Society. Biomimetic Pitcher Plant is adapted with permission.<sup>[42]</sup> Copyright 2019, American Chemical Society. Biomimetic shark skin is adapted with permission.<sup>[43]</sup> Copyright 2007, AIP Publishing. Biomimetic crab is adapted with permission.<sup>[44]</sup> Copyright 2014, American Chemical Society.

### 2.1.1. Lotus Leaf

The well-known, highly water-repellent character of the lotus leaf is a result of its hierarchical microstructure. It consists of 10  $\mu\text{m}$  cone-like features, each decorated with many waxy nanometer-sized hairs (Figure 3). The air trapped inside the cavities, located between the convex-shaped cones, prevents the penetration of water and minimizes wetting. This, acting in unity with the waxy hairs, renders the leaf's surface superhydrophobic. The superhydrophobicity of the surface causes water to bead up when it hits the surface and will consequently roll off the leaves. While rolling, the water droplets collect and remove contaminants from the surface, demonstrating the self-cleaning effect.<sup>[2,19]</sup> However, the lotus leaf loses its superhydrophobicity, and therefore its self-cleaning properties, once the waxy hairs on the outside are lost or when the surface is wetted by long-term immersion in water.<sup>[4,19,45]</sup> Inspired by the lotus effect, Haghdoost and Pitchumani developed superhydrophobic copper coatings, containing 10–20  $\mu\text{m}$  cauliflower-shaped surface features (Figure 3). These densely branched structures were extremely nonwetting, as water did not leave the syringe tip when held against the surface.<sup>[41]</sup> Many more hierarchical superhydrophobic structures have been developed based on the lotus leaf, and are described extensively by several other review articles.<sup>[35,46,47]</sup> Unfortunately, despite its development in many research labs, such hierarchical superhydrophobic surfaces are often plagued by several limitations, including repellency only toward high surface tension liquids, low mechanical stability, weak pressure stability, low transparency, and short-term underwater stability.<sup>[48]</sup> To overcome some of these potential drawbacks, bioinspired SLIPS have been proposed as a possible solution, which will be covered in the next section.

### 2.1.2. Pitcher Plant

While the lotus leaf uses its air-filled microstructure to repel water, the microstructure of the carnivorous *Nepenthes* pitcher plant actually traps water, resulting in a slippery coating.<sup>[49]</sup> The surface of the plant's upper rim, known as the peristome, consists of a well-organized hierarchical microstructure, formed by overlapping epidermal cells (Figure 3).<sup>[38]</sup> This peristome surface is completely covered with a layer of hydrophilic nectar. Therefore, water droplets quickly fill the pores to form a homogeneous liquid film on top, making the peristome surface highly slippery. Once an insect steps onto the peristome, it loses its grip and slides into the digestive juices at the bottom.<sup>[38]</sup> Based on this knowledge, biomimetic pitcher-like surfaces, known as slippery liquid-infused porous surfaces (SLIPS), were developed. Just like the pitcher plant, SLIPS consist of a micro- or nanostructured surface that is capable of locking a film of lubricating liquid into place. This way, SLIPS are able to repel a wide variety of immiscible liquids and solids, thus providing antifouling and self-cleaning properties.

The Aizenberg group prepared such SLIPS coatings by impregnating a nanoporous substrate (e.g., PTFE or an epoxy resin) with a nonvolatile and immiscible perfluorinated liquid.<sup>[50]</sup> The substrate was functionalized with a polyfluoroalkyl silane, to facilitate efficient wetting of the

substrate by the fluorinated oil. Obviously, the oil should be immiscible with any liquid that the coating will be exposed to. Tuning of these parameters resulted in surfaces that strongly repelled both aqueous and organic formulations. Furthermore, solid particles (like carbon and glass dust) could be easily removed by simply rinsing with water. In collaboration with the Miserez group, SLIPS was also demonstrated to be effective against marine fouling, in particular against mussel adhesion.<sup>[51]</sup> Two methods were used to prepare SLIPS coatings: 1) poly(dimethylsiloxane) (PDMS) networks that were impregnated with silicone oil and 2) silica nanoparticle/oil coatings formed via layer-by-layer (LbL) deposition. Compared to non-infused controls and commercial PDMS- and fluoropolymer-based fouling-release coatings, tests in real-world situations revealed both strategies to resist mussel attachment far better, and adhered mussels were much easier removed.

Fabrication of ultraslippery coatings is not limited to polymeric materials. Wang et al. prepared nanostructured titanium alloy surfaces through anodic oxidation of a Ti-6Al-4 V precursor (i.e.,  $\text{Ti}_{0.9}\text{Al}_{0.06}\text{V}_{0.04}$ ).<sup>[52]</sup> The SLIPS functionality was subsequently introduced through fluorosilane surface modification and impregnation with a perfluoropolyether (Figure 3). Compared to the untreated alloy, the slippery titanium surface reduced and weakened attachment of both diatoms and bacteria. Since titanium alloys are already widely employed in the marine industry because of their excellent corrosion resistance, this could be an ideal method to introduce antifouling properties as well.

A significant advantage of the SLIPS strategy over other coating technologies is its ability to restore the antifouling properties after damage, as the repellent liquid will be able to refill the voids. However, due the required capillary action, this self-healing capability is limited to micrometer-sized scratches: large-area physical damage is irreversible, leading to loss of the surface's antifouling properties. Instead of using fragile textured surfaces, thick bulk-porous coatings could lower the sensitivity to abrasion. The fluoropolymer-based SLIPS that were recently reported by the group of Rapp are an excellent example of this approach.<sup>[53,54]</sup>

Another issue that may hinder long-term stability is the loss of the lubricating top layer through evaporation or physical shear. Zhao et al. tackled this problem by blending the silicon oil-based lubricant with a supramolecular PDMS precursor, which caused the lubricant to be stored as discrete droplets inside the bulk material.<sup>[55]</sup> Even when the silicon oil was removed on purpose, the coating's self-replenishing effect led to rapid recovery of the antifouling properties and was maintained for over 300 cycles. This strategy could therefore be applied to prolong the stability of slippery liquid-infused porous surfaces.

### 2.1.3. Marine Organisms

**Shark Skin:** Shark scales are structurally different from most fish scales. Instead of being flat, their tooth-like scales are covered with enamel that is analogous to human teeth, and they have a distinct topography comprised of microscopic ridges arranged in a diamond-like pattern (Figure 3). This unique hierarchical structure and functional roughness give them physical protection against adhesion, as well as excellent drag reduction.<sup>[1,56,57]</sup>

Inspired by the riblet structure of shark skin, Carman et al. were able to develop the well-known biomimetic “Sharklet” antifouling coating (Figure 3). It consists of ordered, well-defined surface features (ridges and pillars) that are typically tailored to the critical dimensions of the fouling organism.<sup>[43,58]</sup> Many researchers have developed improved antifouling coatings by modifying this particular hierarchical design. As an example, Yang et al. fabricated Sharklet surfaces of varying feature heights, terminated with different chemical moieties. They showed that the adhesion strength decreased with increasing feature height and hydrophilicity of the surface, as it reduced the contact area and weakened the foulant-surface interaction.<sup>[31]</sup> To further counteract organism settlement, Munther et al. developed Sharklet-patterned surfaces with an integrated height gradient. This design not only minimized the number of attachment points, but the height difference between neighboring features could also prevent the settlement of organisms inside the gaps.<sup>[59]</sup>

Unfortunately, many studies indicate that additional chemical modification of the shark-like surface is required in order to achieve the desired level of antifouling, since sharks also continuously secrete lubricating and antifouling mucus. Additionally, the best drag reduction and antifouling performance of these biomimetic shark skin surfaces are only obtained when operated in dynamic environments.<sup>[19]</sup>

*Pilot Whale:* The skin of pilot whales exhibits a flat, smooth surface, characterized by a pattern of nanoridge-enclosed pores, with an average pore size of  $0.20\ \mu\text{m}^2$ . Because these pores are smaller than most marine organisms, they reduce the available space for attachment, thereby minimizing biofouling.<sup>[60]</sup> Cao et al. developed a polyelectrolyte multilayer (PEM) coating with a similarly structured surface, obtained through LbL spray-coating deposition of oppositely charged poly(acrylic acid) (PAA) and polyethylenimine (PEI) polyelectrolytes (Figure 3). By tuning the pH of the PEI solution, the topographical properties, including texture size, film roughness and thickness, could be systematically controlled, which subsequently influenced the settlement of fouling organisms. The lowest settlement was observed for structures with a texture size on the order of  $2\ \mu\text{m}$ , which is the same size as the surface features on pilot whale skin.<sup>[32]</sup>

*Sea Urchin:* The spiky surface of the sea urchin presents another unattractive surface for biofoulants, as the densely packed needles prevent any marine life from growing in between the spaces. Gao et al. fabricated biomimetic superhydrophobic sea urchin-like membrane surfaces of poly(L-lactic acid) in order to reduce membrane contamination (Figure 3). The rough, spiky structure contained trapped air, which drastically improved the hydrophobicity compared to the flat control. The superhydrophobicity, together with the reduced contact area of the spiky surface, endowed the membrane surface with self-cleaning properties and suppressed protein and bacteria adsorption.<sup>[40]</sup>

#### 2.1.4. Insects and Shells

For many land-flying insects, including the cicadas and dragonflies, it is known that their wing structure exhibits superhydrophobic properties, which gives them the ability to prevent undesirable microbial adhesion. Moreover, the interaction with natural organic contaminants is further minimized

by their nanostructured surfaces. In fact, when bacteria try to attach to the surface, the nanostructured features are able to penetrate the bacteria's cell membranes, leading to rapid cell rupture and cell death. The cicada and dragonfly wings both possess arrays of nanopillars with heights of  $\approx 200\ \text{nm}$ , but differ in their arrangement (Figure 3). Gangadoo et al. assessed the antifouling capability of these nanostructured wings when immersed in seawater. While each of the structured wings showed an improved resistance to biofouling when compared to a smooth surface, the most disordered surface (based on the dragonfly wings) was most resistant to fouling. It was postulated that the low adsorption properties are related to air trapped at the surface, similar to the lotus leaf.<sup>[4,37]</sup>

The shells of many invertebrates also contain specific microtopographies, including the microripples ( $1.5\ \mu\text{m}$ ) on blue mussels, the spicules on crabs ( $2\text{--}2.5\ \mu\text{m}$ ), knob-like structures ( $10\ \mu\text{m}$ ) on brittle stars and the  $30\text{--}50\ \mu\text{m}$  irregularly wide ridges on the egg-case of dogfishes (Figure 3). Microtopography replicas of these shells, casted in epoxy resin, were able to reduce the fouling for only three to four weeks.<sup>[1,33]</sup> Based on the complex microstructure of crab shells, Yang et al. designed  $3\ \mu\text{m}$  cylinder-shaped microstructures on silicon wafers through reactive ion etching. Unwanted adhesion was reduced up to 70% when compared to a smooth silicon surface.<sup>[61]</sup> Similarly, Brzozowska et al. developed PDMS-based hierarchical replicas of the irregularly structured crab armor via a lithography/casting procedure (Figure 3). The patterned surfaces always outperformed smooth surfaces in adhesion experiments. In addition, the hierarchical patterns turned out to exhibit fouling-release properties, as fouling reduced over time due to hydrodynamic shear forces.<sup>[44]</sup> In an extended study, the combination of the substrate material and surface topography was shown to be equally important. Soft PDMS microstructures demonstrated better fouling-resistant characteristics than smooth PDMS, while maintaining good fouling-release properties. However, patterned hard poly(methyl methacrylate) (PMMA) substrates performed worse than smooth PMMA surfaces (both fouling-resistant and fouling-release), which was likely caused by mechanical trapping of foulants between the small and rigid surface features. Hence, besides surface topography, optimization of surface mechanics and chemistry are also essential for the design of efficient antifouling coatings, which will be the focus of the next section.<sup>[62]</sup>

## 2.2. Chemical Surface Composition

While the physical alteration of microtopography presents a nontoxic, versatile and easy approach to minimize biofouling, its antifouling effect is often too weak, foulant-specific and short-lived to provide efficient protection in the long run.<sup>[33]</sup> Because fouling organisms all have different settlement preferences, the species-dependent antifouling potential of microstructured surfaces often fails to prevent fouling when exposed to various fouling communities.<sup>[32,63]</sup> In fact, surface textures mostly showed to have no effect or even an inclusive effect on fouling. The antifouling capability of structured surfaces could be improved by developing complex hierarchical or irregular texture designs instead of creating regularly arranged geometric



features.<sup>[34]</sup> This strategy could also improve their mechanical robustness. Over time and/or under external constraints, the microstructured surfaces often turned out to be too fragile for long-term application; the microstructures are easily destroyed by a slight finger press or by wiping.<sup>[64,65]</sup> By creating complex surface structures, such as spatial micro–nano hierarchical structures, microscale features would be sacrificed in case of mechanical abrasion, but the nanostructures will remain well protected and fouling repelling.<sup>[65]</sup> Other strategies to improve the mechanical stability, including self-healing mechanisms, organic fillers and crosslinking, are discussed in Section 7.

Hence, microtopography alone is insufficient to prevent fouling. That is why nature makes use of additional strategies to keep surfaces clean from fouling, e.g. by secretion of mucus, waxes or other substances.<sup>[66]</sup> Hence, chemical surface modification, which is based on the chemistry of naturally secreted antifouling substances, presents another approach to weaken or inhibit interactions between substrate and foulant. Surprisingly, many naturally occurring biomolecules also exhibit antifouling properties, including amino acids, peptides, proteins, and polysaccharides.

### 2.2.1. Peptides

Peptides are short proteins, consisting of a chain of 2–50 amino acids. In nature, they can act as hormones, growth factors, enzymes, but also as antimicrobial agents. Surprisingly, certain peptides showed antifouling characteristics, including several metabolites produced by marine bacteria.<sup>[71]</sup> The groups of Chen and Ederth fabricated self-assembled monolayers (SAMs) of biodegradable and ultralow fouling peptides. The peptides were anchored to a gold surface via the (di)sulfide cystamine or cysteine unit (**Figure 4a**) and consisted of negatively and positively charged amino acids, resulting in a strongly hydrated

layer that enabled efficient resistance against protein attachment ( $<0.3 \text{ ng cm}^{-2}$ ).<sup>[68,72]</sup> While peptides appear to be resistant to protein adsorption, they are readily degraded by proteases. A biomimetic alternative, namely peptidomimetic polymers, or peptoids, have a similar protein-like backbone, but lack the hydrogen bond donors. This provides them with an increased conformational rigidity and proteolytic stability compared to natural peptides.<sup>[27]</sup> Dalsin and Messersmith adsorbed such antifouling peptoids to titanium through a short DOPA-functionalized peptide anchor. The peptidomimetic polymer adlayer turned out to be highly resistant to serum protein fouling and cell attachment.<sup>[73]</sup> For more information on the antifouling capability of peptide- and peptoid-based coatings, see Section 4.3.

### 2.2.2. Glycoproteins

Glycoproteins, such as the ones regulating adhesion in blood vessels, are amphiphilic molecules that consist of a hydrophobic peptide backbone decorated with hydrophilic carbohydrate side chains in a bottlebrush-like configuration.<sup>[67,74]</sup> When glycoproteins adsorb to a hydrophobic surface, the exposed glycosylated chains modify the surface chemistry to become strongly hydrophilic, which makes them a potential candidate for the development of antifouling coatings. Lubricin (LUB) is a special type of glycoprotein, found in the synovial fluid of human articular joints. Here, it serves as a highly efficient antiadhesive and boundary lubricant. It consists of a central hydrophilic, negatively charged domain, capped by hydrophobic end-domains.<sup>[67,75–78]</sup> Hence, LUB can be classified as a telechelic ABA triblock copolymer. It is able to self-assemble onto almost any surface via its “sticky” hydrophobic end-domains, while the extended central charged domain endows the surface with antifouling properties. Greene et al. investigated the

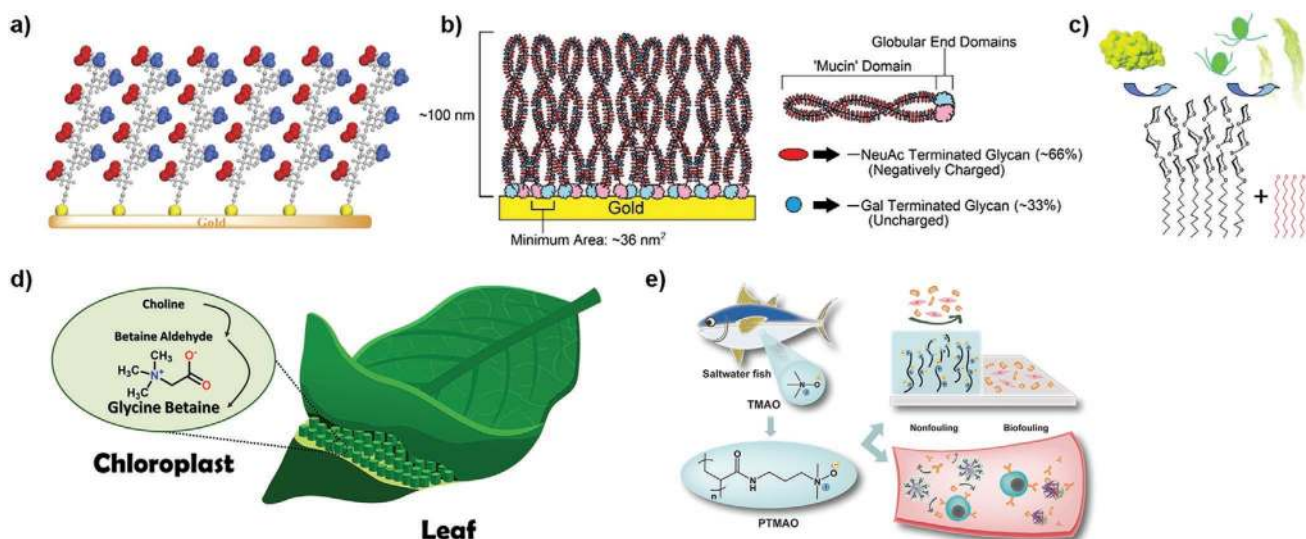


**Figure 4.** Bioinspired synthetic antifouling systems, including a) peptide SAMs, b) lubricin brushes, c) polysaccharide SAMs, d) polyphosphorylcholine derived from glycine betaine, and e) TMAO-derived zwitterionic polymers. (a) Adapted with permission.<sup>[68]</sup> Copyright 2015, Elsevier. (b) Reproduced with permission.<sup>[67]</sup> (c) Adapted with permission.<sup>[69]</sup> Copyright 2011, American Chemical Society. (e) Reproduced under the terms of a Creative Commons Attribution NonCommercial License 4.0.<sup>[70]</sup> Copyright 2019, American Association for the Advancement of Science.

self-assembly and antifouling performance of biomimetic LUB brushes on gold (Figure 4b). The steric repulsion produced by the well-ordered polymer brush-like architecture and the strongly bound hydration layer around the central domain may be the main reasons for its effective antifouling properties and lubricating character.<sup>[67]</sup> However, while the negatively charged domain enables the formation of a strongly bound hydrated layer, rendering the surface antifouling, it also presents one major drawback: these negative charges facilitate nonspecific adhesion of positively charged foulants. In addition, the adsorption of LUB is limited to specific surfaces: when adsorbing LUB on positively charged surfaces, it complicates the ability of LUB to adopt its ideal chain conformation for antifouling purposes.<sup>[79]</sup>

### 2.2.3. Polysaccharides

Polysaccharides are a big culprit of biofilm formation. Being present on the surface of many microbial cells, the extracellular polysaccharides mediate most of the cell-to-cell and cell-to-surface interactions, which are required for formation, cohesion, and stabilization of biofilms. However, recent studies have identified several bacterial polysaccharides that are actually able to inhibit or destabilize biofilm formation, also known as anti-biofilm polysaccharides.<sup>[80]</sup> Cao et al. investigated the resistance to adhesion of three of such polysaccharides when covalently immobilized on glass, including hyaluronic acid (HA), alginate acid and pectic acid.<sup>[81]</sup> Similarly, Fyrner et al. fabricated SAMs of mono-, di-, and trisaccharide-functionalized alkanethiols on gold (Figure 4c).<sup>[69]</sup> In each case, the combination of hydration and steric repulsion makes them resistant to mammalian cells, certain classes of bacteria and marine organisms.<sup>[69,81]</sup>

While these biocompatible and biodegradable polysaccharides were shown to be biofilm-inhibiting, their antifouling performance is highly dependent on the environmental conditions. When immersed in (sea)water, polysaccharides are able to bind divalent ions (calcium, magnesium), which decreases the hydration and entropy of the polysaccharide films. As a consequence, the polysaccharide films are rendered more “attractive”, promoting the undesired adhesion of proteins and cells. Hence, polysaccharide coatings have a decreased fouling resistance when used in marine environments or in other aqueous applications.<sup>[81]</sup>

### 2.2.4. Zwitterionics

Many zwitterionic substances can be found in nature, including phosphorylcholine in cell membranes, taurine in animal tissues and glycine betaine in plants (Figure 4d). These substances have been the inspiration for the successful design of novel ultralow fouling zwitterionic brush surfaces, which involve polyphosphorylcholine, polysulfobetaine, and polycarboxybetaine (PCB). The excellent antifouling performance arises from the electrostatically enhanced hydration.<sup>[70,82]</sup> Another type of zwitterionic molecules, osmolytes, are found in saltwater fishes. Osmolytes are small, soluble organic molecules produced by living organisms for maintaining cell volume, in order to survive extreme

osmotic pressures. Trimethylamine *N*-oxide (TMAO) is a protein-stabilizing osmolyte, and counteracts the effects of protein denaturants, like urea.<sup>[83]</sup> Li et al. showed that their biomimetic TMAO-derived zwitterionic polymer could effectively minimize fouling ( $<3 \text{ ng cm}^{-2}$ ), due to its strong and extensive hydration layer (Figure 4e).<sup>[70]</sup>

The superior antifouling capability, simplicity of synthesis, abundance of raw materials, and ease of functionalization make zwitterionic molecules highly promising for the development of antifouling coatings.<sup>[22]</sup> Yet, zwitterionic polymers are swollen in aqueous media, resulting in poor adhesion to the surface. Consequently, to create a stable zwitterionic surface, extensive surface modification and covalent binding methods are required, which simply cannot be realized on large scales. In addition, the surroundings (e.g., pH, ionic strength, temperature) can strongly influence the antifouling performance of the zwitterionic material. All these factors can limit their final usability in industrial applications.<sup>[84,85]</sup>

To summarize, by using many examples taken from nature, we have shown that both surface chemistry and surface topography affect fouling behavior. Actually, the exceptional antiadhesive properties of many surfaces in nature are the result of a combination of the particular surface chemical composition and hierarchical surface structure. The microstructured skin of sharks, together with the mucus it secretes, reduces bioadhesion as it moves through water. Insects, as well as plants, secrete superhydrophobic compounds on their microstructured surfaces. This synergistic effect has been proposed as an interesting alternative to improve the long-term antiadhesive surface properties of synthetic antifouling surfaces. In the remaining of this work, we will not further elaborate on the synergy between surface chemistry and surface topography, but rather focus on the synergy between different antifouling strategies. This will be covered in Section 6, but first, each antifouling strategy will be introduced.

## 3. Fouling-Resistant Coatings

Fouling-resistant coatings inhibit the settlement of proteins, algae, and/or bacteria.<sup>[1,18–20]</sup> This type of coating mainly relies on modification of the surface chemistry in order to prevent unwanted adhesion. It often involves high interfacial energy surfaces, i.e., highly hydrated surfaces, where strongly coordinated water networks prevent any possibility of attachment or replacement by foulants. Polymer brushes are a versatile tool for adjusting or switching the interfacial energy of surfaces. They can be defined as a densely packed array of polymer chains, end-attached to an interface and stretched out into solution.<sup>[9–12]</sup> They allow facile incorporation of functional groups with antiadhesion, antimicrobial, and anticorrosion properties. Moreover, their high polymer density, often combined with a tightly bound water layer, act as a physical and free energy barrier to keep fouling particles at a distance. Polymer brushes are therefore the focus of this section, and we will try to highlight the most exciting antifouling brushes of the past 5 years.<sup>[3,12]</sup> Yet, the golden standard, polyethylene glycol, must be introduced first, since most state-of-the-art antifouling brushes have emerged from this discovery.



### 3.1. Linear PEG Brushes—The Golden Standard

Currently, grafting polyethylene glycol (PEG) to surfaces (also known as PEGylation) in order to develop linear PEG brushes, is still the standard strategy to resist the adsorption of numerous protein molecules.<sup>[67,70]</sup> PEG is water-soluble, non-toxic, very flexible, biocompatible, has a low immunogenicity, is approved for internal consumption and attains extremely large exclusion volumes.<sup>[9,23]</sup> The reason for its efficient repulsion of foulants has been linked to the extensive hydration layer (and consequently a large excluded volume effect), rapid conformational changes and steric repulsion.<sup>[13,14,92,93]</sup>

Prime and Whitesides were the first to report the superior protein-repelling potential of PEG derivatives, by coating substrates with a SAM of oligo(ethylene glycol). They also found that incorporation of more ethylene oxide (EO) units inside the chains ( $n = 1$  to  $n = 17$ ) led to better resistance to adhesion, as they more effectively covered the surface than the shorter chains did.<sup>[94,95]</sup> After their discovery, many other groups followed by coating various substrates with PEG of different architectures and using several types of grafting techniques. They all showed excellent protein and/or cell resistance, including PEG-tethered surfaces on gold,<sup>[96]</sup> glass-adsorbed poly(2-aminoethyl methacrylate hydrochloride)-PEG copolymer (Figure 5a),<sup>[86]</sup> PEG monomethyl ether grafted to glass surfaces treated with (3-aminopropyl)dimethylethoxysilane and PAA,<sup>[97]</sup> and PEGylated polyaniline nanofibers.<sup>[93]</sup> Moreover, Wu et al. managed to (synergistically) improve the antifouling performance of PEG by incorporation of zwitterionic polymer chains. The PEG chains lowered the electrostatic repulsion between the zwitterionic chains and increased their grafting density on gold

surfaces, while the zwitterionic polymers effectively improved the antifouling performance that was offered by PEG chains alone.<sup>[98]</sup>

While the first-generation antifouling PEGylation method remains most popular for controlling undesired adhesion, it has been found that PEG is readily subjected to oxidative degradation and enzymatic cleavage in most biochemically relevant environments. The cleavage of EO units results in the formation of aldehyde-terminated chains, which can react with amine-functionalized proteins. The short-term stability of PEG therefore limits its protein resistance ability over extended periods.<sup>[22,68,73,99]</sup> More practically, it remains difficult to graft PEG to various chemically different substrates and it often requires the need for complex surface chemistry, which can become very costly during industrial scale-up or when applied to larger substrates.<sup>[67,100]</sup> Additionally, due to their highly hydrated nature, PEG coatings swell in aqueous environments, which compromises their mechanical strength and further restricts their practical feasibility.<sup>[101]</sup> Adsorption of cationic foulants (like lysozyme) presents another weakness of PEG coatings, indicating that PEG is not a universal antifouling material after all.<sup>[102]</sup> Finally, PEG coatings show a weakened protein resistance at higher temperatures (>35 °C), which are critical temperatures for many biomedical applications.<sup>[13,88,92]</sup> This behavior was rationalized by the fact that water is more readily displaced at higher temperatures, and PEG starts to order the water less efficiently. In other words, the coating loses its extensive hydration layer and becomes more hydrophobic.<sup>[103]</sup>

Hence, many groups have started the search for alternatives, including lubricin,<sup>[67,78]</sup> polyoxazolines,<sup>[89,90]</sup> polyglycerol

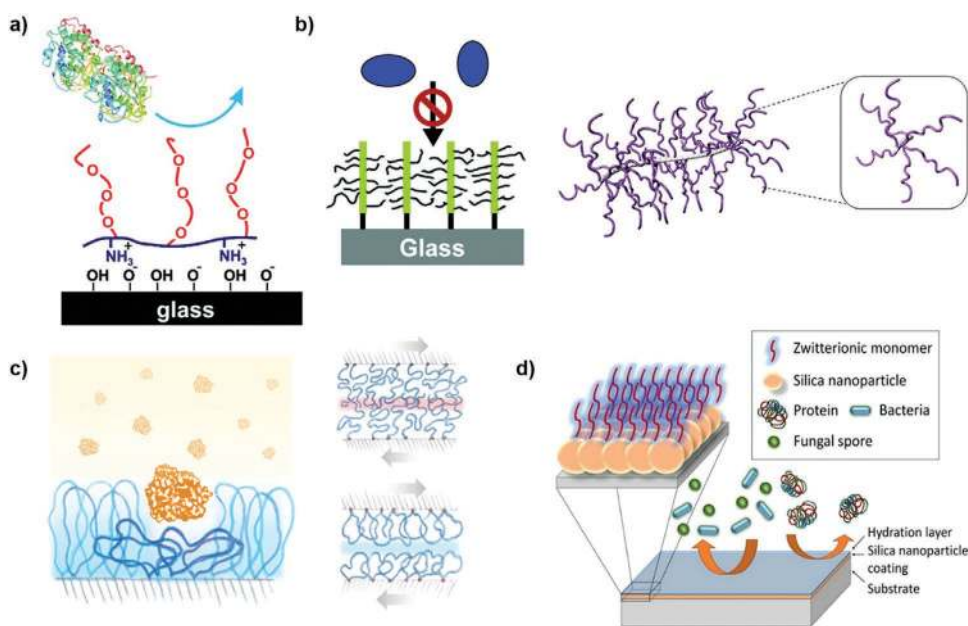


**Figure 5.** Schematic representations of a) linear PEG brushes, b) POEGMA bottlebrushes and its 3D architecture, c) cyclic PEOXA brushes, and d) sulfobetaine-functionalized silicon nanoparticle brushes. (a) Adapted with permission.<sup>[86]</sup> Copyright 2010, American Chemical Society. (b) Adapted with permission.<sup>[87,88]</sup> Copyright 2006, American Chemical Society, and, Copyright 2012, American Chemical Society. (c) Adapted with permission.<sup>[89,90]</sup> Copyright 2017, American Chemical Society, and, Copyright 2016, Wiley-VCH. (d) Reproduced with permission.<sup>[91]</sup> Copyright 2017, American Chemical Society.

dendrons,<sup>[104,105]</sup> polyvinylpyrrolidone (PVP),<sup>[106]</sup> polysaccharides,<sup>[3,80]</sup> polypeptoids,<sup>[73,107]</sup> polyacrylamide<sup>[108,109]</sup> and zwitterionic polymers.<sup>[82,91,99]</sup> These alternatives can show similar or sometimes even better resistance toward fouling. Several of these alternatives will be introduced in the next sections.

### 3.2. Bottlebrushes

While recent efforts into the design of antifouling polymer coatings have primarily focused on linear polymer brushes (like PEG), bottlebrush-coated surfaces actually show superior protein resistance. Bottlebrush polymers are similar to linear polymers, but the backbone is decorated with densely packed polymeric side chains. This type of architecture creates a denser and even more impenetrable layer, resulting in an exceptional antifouling capability.<sup>[88,110,111]</sup>

Wang et al. demonstrated the superior antifouling ability of PVP bottlebrush surfaces over linear PVP brush surfaces, at similar polymer layer thickness and grafting density. The PVP bottlebrushes strongly reduced adsorption of several proteins compared to both bare gold surfaces (up to 97%) and linear PVP brush-coated surfaces (up to 44%). Since the grafting density was similar, the superior resistant property of the PVP bottlebrush can only be explained by its smoother and denser impenetrable layer.<sup>[106]</sup> Joh et al. studied the antifouling capability of poly[(oligoethylene glycol) methyl ether methacrylate] (POEGMA) bottlebrushes, a PEG derivative (Figure 5b).<sup>[110]</sup> When the film thickness of these brush coatings was larger than 14 nm, they provided complete protein resistance to fibronectin, bovine serum albumin and lysozyme on a wide range of substrates (gold, glass, (polymer-coated) silica).<sup>[87,111,112]</sup> Most notably, the level of serum adsorption on these coatings was below the 0.1 nm detection limit of ellipsometry and no fluorescence from attached cells could be observed.<sup>[87,111]</sup>

Another interesting bottlebrush building block involves the polyoxazoline family, poly(2-methyl-2-oxazoline) (PMOXA). It has many interesting properties, including resistance to oxidative degradation, less demanding synthesis, noncytotoxicity and similar protein-repellent properties as PEG-based materials.<sup>[113,114]</sup> Based on this knowledge, Zheng et al. spin-coated gold surfaces with thiol end-capped poly(methacrylic acid)-g-poly(2-methyl-2-oxazoline) (PMAA-g-PMOXA) bottlebrush polymers, which exhibited good protein resistance and excellent anti-platelet adhesion compared to bare gold. They also showed that the protein-resistant properties of the PMOXA bottlebrush could be fine-tuned by varying the lengths of the backbone and side chains: a shorter PMAA backbone and longer PMOXA side chains led to a higher surface coverage, better hydrophilicity, and thus a higher protein resistance.<sup>[114]</sup>

### 3.3. Cyclic Polymer Brushes

Besides PMOXA bottlebrushes, PMOXA has also been studied extensively as cyclic- and loop-structured brushes. Generally, polymers with conformation-constrained architectures, such

as dendrons, loops and cycles, can generate denser brushes and thus show better protein-resistant properties compared to their linear analogs.<sup>[106]</sup> Indeed, the group of Benetti found that cyclic polymer brushes outperform the lubricating and biopassive properties of their linear counterparts (Figure 5c). They developed multiple cyclic polymer brushes, mostly based on poly(2-alkyl-2-oxazoline)s, such as PMOXA and poly(2-ethyl-2-oxazoline) (PEOXA). Several factors contribute to the superiority of using cyclic polymers. The smaller hydrodynamic radius of the cyclic macromolecules enables faster adsorption and the fabrication of highly stretched and compact brushes. The high brush density creates an enhanced steric barrier that surpasses the typical entropic shield of a linear brush, therefore preventing the penetration of biomolecules more efficiently. Additionally, the absence of dangling chain ends at the brush interface suppresses intercalation when two brush-functionalized surfaces are sheared against one another, resulting in a lubricin-like lubrication.<sup>[89,90,113]</sup>

Despite the unique features of these cyclic polymer brushes, to obtain the cyclic polymers in large quantities and high purity is still very costly and complex. This, together with the surface modification techniques required to obtain highly dense and chemically stable brushes, limits their suitability for large-scale applications.<sup>[115]</sup>

### 3.4. Nanoparticle Thin Films

Besides linear, bottle and cyclic polymer brushes, there is another method to develop antifouling brushes, namely by coating surfaces with “hairy” nanoparticles (NPs) (Figure 5d). Knowles et al. spin-coated thin films of zwitterionic sulfobetaine (SB)-functionalized silica NPs onto a gold substrate to generate hydrophilic coatings that demonstrated excellent fouling-resistant properties against protein, bacterial and fungal spore adhesion. Three different methods were used for preparing zwitterionic SB-modified surfaces: grafting SB to a SiO<sub>2</sub> substrate, grafting SB to the silica NP thin film on gold, and grafting SB to silica NPs in suspension and subsequently depositing them on gold. While protein adsorption and bacterial adhesion on SB-functionalized silica NP surfaces were significantly reduced compared to unfunctionalized silica NP coatings (up to 96%), it was unable to provide the same level of resistance compared to SB coatings on plain SiO<sub>2</sub>. Even though the NPs did not show an enhanced antifouling performance, they do have advantages. Particle functionalization and coating fabrication can easily be carried out in an aqueous solution across a wide pH range and on various substrates, without the need for a catalyst. The materials are cheap, highly processable, and the chemical processes are easily scalable and do not require organic solvents or surface treatments, which makes them very attractive for widespread antifouling applications.<sup>[91]</sup>

## 4. Fouling-Release Coatings

While a perfect fouling-resistant coating should completely prevent the attachment of foulants, weak adhesion is still permitted in fouling-release coatings.<sup>[3]</sup> Due to a weak interaction

with the surface, the foulant can be easily removed through hydrodynamic shear or a simple mechanical cleaning step. The more classical approaches often rely on strongly hydrophobic surfaces, although in the past two decades more advanced technologies based on amphiphilic coatings, peptides/peptoids and composites have been presented. Such approaches will be introduced in the upcoming sections, and recent and exciting strategies will be highlighted.

#### 4.1. Hydrophobic Surfaces

The implementation of hydrophobic materials in fouling-release coatings already dates back to the 60s and 70s of the last century. These coatings are only able to interact with the environment through dispersive forces; polar interactions (like hydrogen or ionic bonds) should be avoided at all times. Settlement of amphiphilic biofoulants is still possible, but as a consequence of these weak interactions, they can usually be easily removed afterward. Since fouling of hydrophobic surfaces is inevitable, it should be pointed out that pure fouling-release coatings can only be successfully applied in dynamic environments, meaning that the surfaces should be regularly subjected to hydrodynamic shear forces.<sup>[120]</sup>

Efficient fouling-release coatings are typically based on materials that 1) have a low surface energy, 2) have a low modulus (to facilitate detachment), and 3) form a smooth surface (to avoid mechanical interlocking).<sup>[121]</sup> Fluorinated polymers and silicone elastomers meet these requirements remarkably well, and therefore their fouling-release performance has been thoroughly investigated by various research groups. Despite the high chemical stability of both polymer types (in contrast to PEG in fouling-resistant coatings, see Section 3.1), both materials have their limitations. For example, polytetrafluoroethylene (PTFE) was initially considered as a good candidate for fouling-release coatings, but turned out to be easily damaged, leading to rapid and irreversible fouling via mechanical interlocking (i.e., foulants physically bind to the irregularities of the damaged surface). Additionally, PTFE is difficult to process (due to its low solubility and high crystallinity) and it is difficult to attach to surfaces.<sup>[121,122]</sup> The interest in fluoropolymers therefore shifted to other fluorine-containing polymers, such as fluorinated (meth)acrylates and perfluoropolyethers. A very interesting alternative approach was suggested by Krishnan et al., which encompassed fluorinated comb-shaped liquid crystalline block copolymers.<sup>[123]</sup> In this work, the liquid crystalline phase prevented surface reorganization, whereas the polystyrene block acted as a compatibilizer and provided solubility to the system.<sup>[26]</sup> Compared to a hydrophilic fouling-resistant PEG analogue, the sporelings release performance of this fluorinated copolymer turned out to be better, but worse in case of diatoms. These results demonstrate the high importance of specific organism-surface interactions.

Similarly, a limitation of PDMS elastomer coatings is their poor mechanical stability and weak adhesion to substrates and primers. The group of Webster tackled these problems by preparing siloxane-polyurethane (PDMS/PU) hybrid coatings that contained up to 30 wt% PDMS: the major PU component provided tough bulk properties and better substrate adhesion,

while a PDMS surface was spontaneously formed during film formation (i.e., self-stratification).<sup>[124,125]</sup> The high crosslinking density prevented surface reconstruction when the material was immersed in aqueous media, resulting in a fouling-release performance that was comparable to existing commercial systems. Lubrication of the surface via incorporation of silicone oils led to even further enhanced properties (Figure 6a).<sup>[116]</sup> As little as 1 wt% of oil already turned to be highly effective: reduced adhesion and improved release was observed for macroalgae, barnacles and mussels.

Besides blending PDMS with stiffer polymeric materials, like PU in previous examples, the mechanical properties of silicone-based fouling-release coatings may also be improved by the addition of inorganic fillers. Such organic/inorganic composites are, however, accompanied by several other challenges, and are therefore covered in a separate section (Section 4.4).

From a chemical and processing point of view, PDMS-based coatings are also plagued by various obstacles, which include the use of heavy metal-based catalysts, long reactions times, and the requirement of a final heating step to complete the condensation and hydrosilylation reactions. To overcome these problems, Martinelli et al. proposed an alternative strategy that involved room temperature photo-crosslinking of methacrylic PDMS oligomers by UV light, without requiring any toxic catalysts.<sup>[126]</sup> Besides being a faster and more environmentally friendly method, this route also allowed facile adjustment of the fouling-resistant and fouling-release properties by simple addition of PEGylated or fluorinated methacrylic co-monomers. Surface reconstruction was observed for several of such binary or ternary compositions upon contact with water, which may have a severe effect on the fouling-release properties.

#### 4.2. Amphiphilic Surfaces

Despite the absence of polar interactions, certain foulants still strongly adhere to hydrophobic surfaces. As soon as they have attached, water is required to penetrate the favorable coating/foulant interface, while simultaneously the unfavorable coating/water interface has to be recreated. These processes will hinder the removal of foulants.<sup>[127,128]</sup> Attachment via either hydrophobic or hydrophilic interactions can be discouraged through inclusion of hydrophilic moieties within a hydrophobic coating, leading to spontaneous formation of nanoscale heterogeneities. Such mixed hydrophobic/hydrophilic surfaces will result in reduced initial growth (i.e., fouling-resistant) and improved fouling-release properties. To this end, multiple research groups have prepared amphiphilic coatings by combining fluoropolymers with PEG, either in the form of hyperbranched crosslinked networks,<sup>[129]</sup> perfluoropolyether networks,<sup>[130]</sup> or even mixed with PDMS to generate fluoro/siloxane/PEG hybrid coatings.<sup>[131]</sup>

More recently, Galhenage et al. developed PEG-modified PDMS/PU amphiphilic coatings within a single synthesis step, which was accomplished by reacting a PU prepolymer with end-functionalized PEG and PDMS.<sup>[132]</sup> The isocyanate trimer brought the hydrophilic and hydrophobic components together and caused these to phase separate into micrometer-sized domains that aggregated near the water/coating interface. While only 10 wt% PEG/PDMS was incorporated in these PU



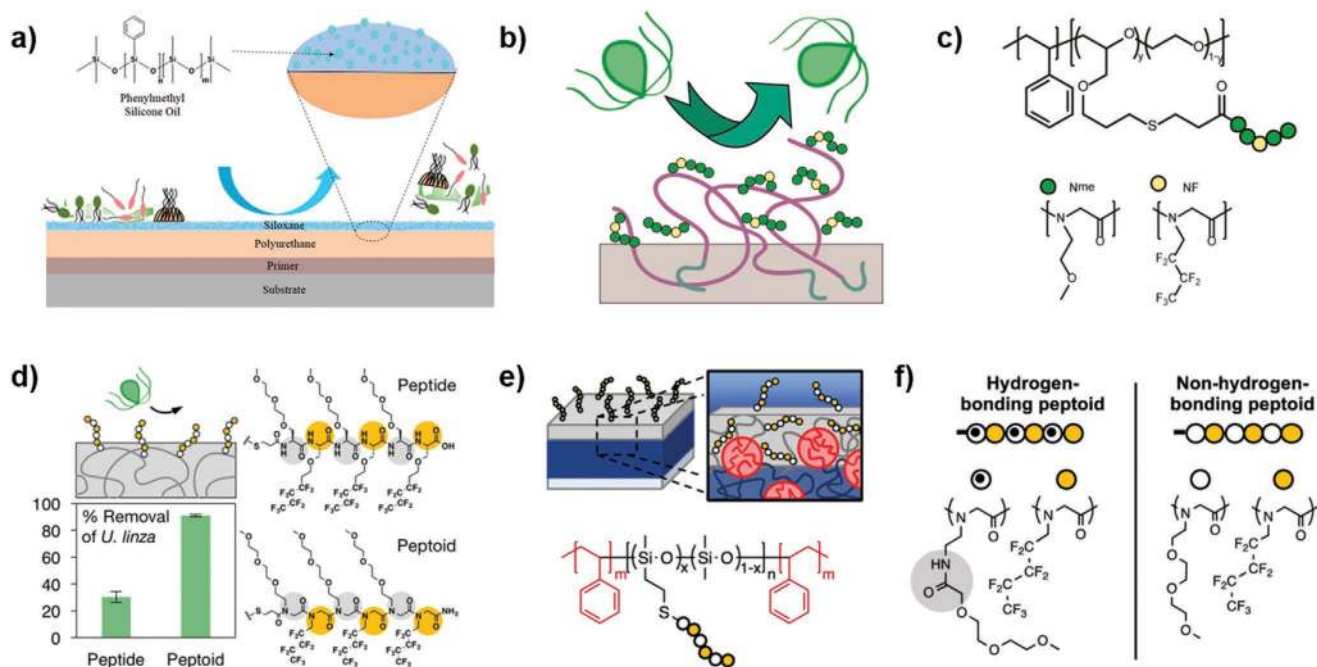


**Figure 6.** a) In PDMS/PU blends, self-stratification resulted in a multilayered fouling-release coating that demonstrated a higher efficiency compared to conventional silicone oil-infused PDMS coatings. Reproduced with permission.<sup>[116]</sup> Copyright 2016, American Chemical Society. b) Schematic representation of an amphiphilic peptoid-modified PS-*b*-P(EO-*co*-AGE) coating, and c) their chemical structures. Adapted with permission.<sup>[117]</sup> Copyright 2014, American Chemical Society. d) Enhanced fouling-release properties were observed compared to peptide-functionalized copolymers. Reproduced with permission.<sup>[118]</sup> Copyright 2017, American Chemical Society. e, f) Design of a hydrogen-bond-donating peptoid confirmed the lack of H-bonding units to be responsible for this behavior. Adapted with permission.<sup>[119]</sup> Copyright 2019, American Chemical Society.

coatings, excellent fouling-release properties against a broad spectrum of organisms were obtained, that even outperformed several commercial standards. Addition of PEG led to a further improvement of the in Section 4.1 introduced hydrophobic PDMS/PU coatings.

Still, the preparation of multicomponent amphiphilic nanostructured fouling-release coatings can be quite challenging, as it may be difficult to find the right balance between hydrophobic and hydrophilic interactions, and macroscopic phase separation should always be prevented. Block copolymers are ideal macromolecular materials to overcome these limitations, since they allow excellent control over the amphiphilic properties, whereas their architecture guarantees the formation of nanometer-sized hydrophobic and hydrophilic domains.<sup>[120]</sup> As an example, the Ober group has extensively investigated the fouling-release properties of coatings based on modified polystyrene-*block*-poly(ethylene-*ran*-butylene)-*block*-polyisoprene (PS-*b*-P(E/B)-*b*-PI) triblock terpolymers. Here, the PS and P(E/B) blocks provided elastomeric properties, while the unsaturated bonds in the PI block enabled facile introduction of hydrophilic and hydrophobic functionalities. Examples of such functionalities include combinations of short PEG and semifluorinated side chains,<sup>[133]</sup> but also fluorine-free nontoxic systems based on PEG,<sup>[134]</sup> PEG/PDMS<sup>[127]</sup> or PEG combined with short hydrophobic alkyl segments.<sup>[135,136]</sup> All variations demonstrated a significantly improved fouling-release performance compared to conventional silicone resin-based fouling-release coatings.

Since the preparation of suitable surface-active block copolymers is typically limited to the gram scale, in particular due to

the required postmodification steps, it will be difficult to scale up these materials from the laboratory stage to commercialized products. Recent studies, however, have demonstrated that when such block copolymers are mixed with either thermoplastic elastomers<sup>[137]</sup> or PDMS resins,<sup>[138]</sup> the fouling-release performance still surpassed the neat control samples and was often very similar to the pure block copolymer coating. These findings were caused by the tendency of the block copolymer's functional groups to migrate to the surface during processing. By using this approach, the required amount of copolymer could be reduced to less than 15 wt%.

### 4.3. Peptides and Peptoids

Whereas block copolymers readily give access to amphiphilic fouling-release surfaces, incorporation of peptides via solid-phase synthesis techniques provides more precise control over the monomer sequence, and thereby the spacing of the hydrophilic and hydrophobic groups.<sup>[139]</sup> The potential of such a biomimetic approach was demonstrated by Calabrese et al.<sup>[140]</sup> To this end, the PDMS block of a PS-*b*-PDMS diblock copolymer was decorated with a mixture of alkylated and PEGylated artificial oligopeptides. Without extensive optimization, these comb-shaped peptide-containing copolymers already demonstrated significantly better fouling-resistant and fouling-release performances than the unmodified diblock copolymer. Although the fouling-release efficiency was reduced compared to a traditional PDMS elastomer, the authors stressed that

far less foulant had to be removed from the peptide-modified coating.

Since peptides remain expensive and challenging to synthesize, focus shifted to biomimetic peptoid-based coatings instead. These poly(*N*-substituted glycine) derivatives involve less complex chemistry, demonstrate a higher solubility due to the reduced number of intra- and intermolecular hydrogen bonds, and are less prone to enzymatic degradation, making them more suitable for use in biological environments. Van Zoelen et al. were one of the first to report the surface properties of such peptoid-containing coatings.<sup>[141]</sup> Surface reconstruction was very sensitive to the number of hydrophobic units: when moving from three to five fluorinated monomers (out of 45), reconstruction became one order of magnitude slower. The influence of this rate on the fouling-release properties turned out to be significant and was studied systematically via a slightly different platform: peptoid-grafted polystyrene-*b*-poly(ethylene oxide-*co*-allyl glycidyl ether) (PS-*b*-P(EO-*co*-AGE)) with different lengths and compositions were synthesized, where the PS block provided mechanical stability to the film (Figure 6b,c).<sup>[117]</sup> Because the fluorinated groups could drag whatever neighbor to the surface (either polar or nonpolar), their position within the sequence changed the surface chemistry and thereby the fouling-resistant properties. The fouling-release properties, on the other hand, were only affected by the number of fluoro monomers.<sup>[142]</sup> Incorporating the hydrophobic peptoid units more toward the middle of the sequence resulted in a more hydrophilic and stronger hydrated surface, and thus better fouling-resistant properties. Better fouling-release properties were observed for coatings that contained less fluoro monomers, because these sequences facilitated faster surface reconstruction and were consequently able to adapt more efficiently to changes in the environment.

Although peptoids are easier to synthesize and process, one may argue that the different backbone structure could have an impact on the fouling-release properties as well. A direct comparison of peptide- and peptoid-containing amphiphilic block copolymer coatings was described by Patterson et al.<sup>[118]</sup> The peptoid-based coatings demonstrated a superior fouling-release performance, which was hypothesized to be caused by the absence of hydrogen bond donors in the polymer main chain, resulting in a weaker adhesion of foulants (Figure 6d). Barry et al. confirmed these results through clever design of a hydrogen-bond donating peptoid block, which was clearly outperformed by the nonhydrogen-bonding analogue (Figure 6e,f).<sup>[119]</sup>

Because peptides and peptoids allow exceptional control over the polymer architecture, these systems are ideal for studying the parameters that determine the fouling-release performance. The molecular weight, composition and sequence all play a crucial role, demonstrating the complexity of amphiphilic coatings. Unfortunately, the high costs, toxic reagents, and lack of scalability of the involved solid-phase methods will hinder mass production.<sup>[143,144]</sup> Even though recombinant or liquid-phase synthesis techniques may overcome some of these limitations, additional postmodification steps are still necessary that are currently only possible on a lab scale. It is therefore not expected that peptide- and peptoid-containing block copolymer coatings become commercially relevant on the short term.

#### 4.4. Organic/Inorganic Hybrid Composites

Besides purely organic and molecularly mixed coatings, several research groups have investigated the fouling-release performance of organic/inorganic hybrid composites, by blending in nano- or micrometer-sized inorganic fillers.<sup>[122,145]</sup>

Qiu et al. reinforced a PDMS/polythiourethane (PTU, a more environmentally friendly alternative to PU) with ZnO microparticles.<sup>[146]</sup> Up to 5 wt% filler material, the particles were homogeneously distributed throughout the PDMS/PTU film. Incorporation of ZnO reduced the coating's hydrophobicity and improved the mechanical stability. All samples, including the pristine PDMS and PTU control samples, showed comparable fouling by algae, mussels, and barnacles when immersed in seawater for 12 months. However, the PDMS/PTU/ZnO hybrid composite demonstrated a significantly higher mechanical durability; foulants could be easily removed without damaging the surface.

Fouling-release nanocomposites based on CuO<sub>2</sub> nanocubes were recently examined by Selim et al.<sup>[147]</sup> When combined with PDMS, smooth films containing a filler loading of up to 5 wt% could be cast from solution. Increased hydrophobic character and effective fouling-release properties were already observed for coatings that contained as little as 0.1 wt% CuO<sub>2</sub> nanocubes. Above 5 wt%, the particles were found to aggregate, resulting in a higher surface roughness and consequently a declining performance. Similar results were later achieved by the incorporation of other superhydrophobic nanofillers, including TiO<sub>2</sub>-SiO<sub>2</sub> core-shell nanorods,<sup>[148]</sup> MnO<sub>2</sub> nanorods,<sup>[149]</sup> and silicon carbide nanowires.<sup>[150]</sup> Besides improving the mechanical stability of PDMS, such an approach could potentially reduce the costs as well.

Whereas PDMS mixed with silicon oils is known to reduce the adhesion strength of foulants (see Section 4.1), it simultaneously softens the film.<sup>[151]</sup> Ba et al. reinforced such lubricated coatings with micrometer-sized granular inorganic particles. This approach indeed led to enhanced mechanical properties. However, diffusion of the silicone oil from the bulk material toward the surface was reduced, which gave rise to a lowered fouling-release performance, regardless of the chemistry of the filler (e.g., CaCO<sub>3</sub>, ZnO, Fe<sub>2</sub>O<sub>3</sub>, or Cu<sub>2</sub>O). When exchanging the filler for a blend of Fe<sub>2</sub>O<sub>3</sub> and multiwalled carbon nanotubes (Fe<sub>2</sub>O<sub>3</sub>/MWCNT), both the mechanical properties and diffusion of silicone oil were improved.<sup>[152]</sup> Here, Fe<sub>2</sub>O<sub>3</sub> was added to avoid shrinkage of PDMS during curing, while the MWCNTs were able to form diffusion channels throughout the film. This effect caused the transport of oil to switch from molecular network diffusion to channel diffusion. Despite the increasing surface roughness with filler concentration, the enhanced diffusion resulted in more efficient biofouling detachment.

Overall, the stiffness of PDMS-based coatings can be improved through addition of micro- or nanometer-sized fillers. The concentration is, however, in most cases limited to only a few percent. Particle aggregation is frequently observed at higher concentrations, leading to an increased surface roughness and consequently a declining antifouling performance. Still, even small amounts of filler can already have a positive impact on both the durability and fouling-release properties, and it may simultaneously reduce the costs of the coating as

well. Traditional fouling-release technologies may therefore benefit from such a hybrid approach.

## 5. Fouling-Degrading Coatings

In contrast to resistant and release coatings, where the foulant remains unaffected by the substrate, fouling-degrading coatings aim to disrupt their adhesive mechanism or even kill the fouling species when they come too close to the functionalized surface.<sup>[27]</sup> Degrading coatings focus especially on the prevention of biofouling, and can either disrupt the cell membrane of the fouling organism, degrade its secreted bioadhesive, interfere cell communication, or break down the extracellular matrix, all eventually leading to foulant removal.

Depending on their way of operation, fouling-degrading systems can be categorized as either contact-killing or (antibacterial) agent-releasing surfaces. In the first approach, biocidal groups are anchored to the surface that degrade or kill the foulant upon contact, while in the second approach a compound is eluted that already disrupts potential foulants before attachment can even occur.<sup>[153]</sup> Applications of fouling-degrading coatings are mostly focused on healthcare (e.g., bandages, orthopedic devices, dental implants) and aim to avoid attachment of bacteria that can cause inflammatory responses.<sup>[154]</sup> Additionally, since such microfoulants play a key role in biofouling, fouling-degrading coatings are promising for use in the food packaging and marine industry as well.<sup>[155]</sup>

Several approaches for introducing fouling-degrading properties into a coating will be discussed in the upcoming sections, and include coatings based on quaternary ammonium compounds, metallic (nano)composites, enzymatic coatings, and photoactive materials.

### 5.1. Quaternary Ammonium Surfaces

Quaternary ammonium compounds are among the most studied materials for use in contact-killing coatings. Surfaces decorated with such functional groups can be prepared through alkylation of an amine-containing material. Attraction between the positively charged ammonium groups and negatively charged cell membranes will cause the single-celled organisms to be dragged toward the surface.<sup>[156,157]</sup> Upon contact between both components, the strong electrostatic interaction will ultimately result in fatal damage of the cell structure.

Multiple innovative strategies have been reported to introduce quaternary ammonium functionalities onto surfaces, including examples like antibacterial PEI paint additives,<sup>[158]</sup> biobased polyphenols for use in catheters,<sup>[159]</sup> and antifogging semi-interpenetrating polymer networks for use in medical optics.<sup>[160]</sup> Still, one of the most popular methods in the scientific community involves quaternary ammonium brushes that are directly grafted from the substrate.<sup>[161,162]</sup> Surfaces with substantial antimicrobial capacities (i.e., >99% cell death within 1 h) can for instance be prepared by polymerizing dimethylaminoethyl methacrylate from a glass or paper substrate, followed by quaternization of the tertiary amino groups.<sup>[163]</sup> However, since this technique requires surface treatment and subsequent

immobilization of the polymerization initiator, upscaling may be expensive and unpractical (see Section 7.2).

The groups of Busscher and Loontjens presented a slightly less exhaustive method to introduce surface-anchored quaternary ammonium groups: hyperbranched polyureas were covalently attached to either glass or PDMS, and were subsequently functionalized with PEI.<sup>[164–166]</sup> This procedure guaranteed high quaternary ammonium densities after alkylation, thereby resulting in excellent bactericidal activities with contact-killing efficiencies of over 99%. In a later study, these hyperbranched polyureas were used as emulsifiers to prepare antimicrobial waterborne paints.<sup>[167]</sup> Despite the translation from functionalized surfaces to PMMA-based paint formulations, the antibacterial properties were preserved, and in addition, the coatings were found to be effective against fungi as well. In contrast to the previously discussed examples, application of such paints does not require any surface pretreatment. Therefore, this method represents a more practical and environmentally friendly approach.

Instead of the more traditional brush-type coating technologies, Yue et al. incorporated antimicrobial functionality in 3D-printable resins for use in dentistry applications (Figure 7a,b).<sup>[168]</sup> This 3D-printable antimicrobial material was obtained by copolymerizing a photocurable resin mixture in the presence of a quaternary ammonium-modified methacrylate monomer. Since photopolymerization is never complete, leaching of unreacted monomers from the composite was observed for up to 6 days. While this may not necessarily lead to biological consequences, leaching was further reduced by exchanging the quaternized monomer for a linear cationic polymer. Optimization of the formulation resulted in bacterial contact-killing efficacies of over 99%. This approach is not limited to dentistry, as 3D-printed antimicrobial materials may be easily transferred to other application areas, like medical devices and food packaging.

A significant disadvantage of quaternary ammonium-functionalized coatings is that such surfaces will eventually become contaminated with the remains of dead microorganisms, which in turn will promote further fouling.<sup>[169]</sup> Consequently, the active top layer will be blocked, leading to rapid reduction of the fouling-degrading performance. These problems may be overcome by incorporation of additional antifouling strategies to obtain a synergistic coating (see Section 6).

### 5.2. Metallic (Nano)Composites

The antimicrobial properties of silver-containing composites were already recognized by several ancient civilizations and therefore count as one of the oldest fouling-degrading strategies. Because of its wide antimicrobial spectrum, silver (Ag) found its way to multiple sectors, including the medical field, personal care products, dentistry and even household items.<sup>[173]</sup> As a releasing agent, Ag(I) ions (either directly or formed through oxidation of metallic silver) are already highly effective at very low concentrations (<1  $\mu\text{g mL}^{-1}$ ) and can also be used to combat antibiotic-resistant bacteria.<sup>[174]</sup> Although the exact mechanism is not yet fully understood, it is evident that multiple actions are responsible for their biocidal activity: Ag(I)



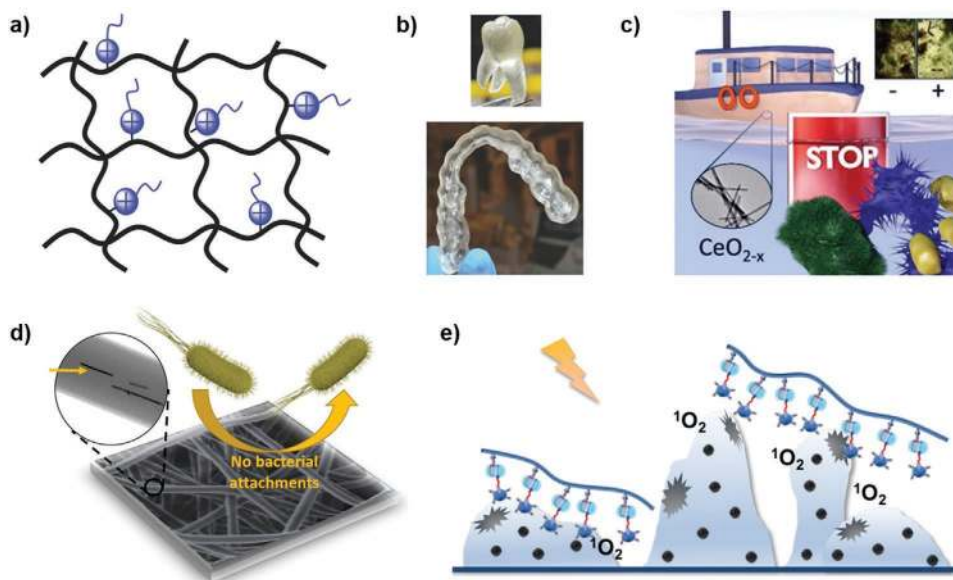


**Figure 7.** a) Photocuring of a quaternary ammonium resin resulted in polymer networks with antimicrobial properties. b) 3D-printing of such resins was applied to prepare dental implants. Adapted with permission.<sup>[168]</sup> Copyright 2015, Wiley-VCH. c) Incorporation of  $\text{CeO}_{2-x}$  nanorod-based artificial enzymes introduced fouling-degrading properties to marine coatings and d) electrospun polymer fabrics. Reproduced with permission.<sup>[170]</sup> Copyright 2017, Wiley-VCH. Adapted with permission.<sup>[171]</sup> Copyright 2018, American Chemical Society. e) Schematic illustration demonstrating the photocatalytic activity of a supramolecular porphyrin-containing polymer. Reproduced with permission.<sup>[172]</sup> Copyright 2019, American Chemical Society.

cations can adhere to the cell membrane and damage the cell structure, bind to the thiol groups of enzymes consequently interfering metabolism, bind to DNA to block the replication cycle, or form reactive oxygen species (ROS).<sup>[153,155]</sup> While one may argue that such a rich biocidal behavior could cause toxic side effects, Vasilev et al. have recently demonstrated that mammalian cells show a significantly greater tolerance to silver than bacteria.<sup>[175]</sup>

Progress in the nanotechnology field caused the research interest in silver-based antimicrobial surfaces to shift from bulk materials to nanoparticles and their composites.<sup>[176]</sup> These nanometer-sized aggregates have a much higher surface area and can cross the body of fouling species to cause intracellular damage. As a result, a comparable fouling-degrading performance can be achieved at lower silver concentrations. Although little is known about the toxicity of Ag nanoparticles, their usage seems to be safe at low concentrations as nanoparticles may be easily eliminated through urine and hair.<sup>[174]</sup> Oliani et al. prepared polypropylene/silver nanocomposites by simple melt extrusion, and added a small amount of polyvinylpyrrolidone to avoid aggregation of the nanoparticles. The composites were nontoxic to mammalian cells, but effectively killed 60–100% of all bacteria at particle loadings of only 1 wt%.<sup>[177]</sup> Similar composites were studied by Cao et al., but focused on their usage in food packaging.<sup>[178]</sup> Excellent antimicrobial and antifungal properties were obtained (>85% cell death), and migration studies demonstrated these composites to be particularly suitable for packaging of watery and alcoholic foods.<sup>[179]</sup>

Other metallic composites, such as based on copper (Cu), have attracted attention as well. Similar to Ag, the precise microbiocidal mechanism of Cu is not fully understood. Two pathways have been proposed: membrane depolarization and

ROS generation.<sup>[180]</sup> Depolarization involves binding of Cu to the membrane, resulting in a decrease of the potential difference between the interior and exterior, eventually leading to cell rupture. In contrast, ROS (e.g., singlet oxygen or hydroxyl radicals) can inflict oxidative damage to the DNA and can readily oxidize attached biomolecules, which will lead to degradation of the pollutants. In contrast to Ag, Cu is active in both its metallic and ionic form, making the antimicrobial activity of Cu-containing coatings much faster and more effective under dry conditions. By using this strategy, Montero et al. showed PMMA/Cu composites to be highly effective against a large library of bacterial cultures (>99.9% reduction compared to control samples).<sup>[181]</sup> Mitra et al. reported an interesting route to prepare transparent Cu-containing coatings that could be used for covering instrument screens in hospitals.<sup>[182]</sup> In this work, polyvinyl fluoride and stainless steel surfaces were functionalized with ligands that could complex to Cu(II) ions. Despite this noncovalent monolayer approach, the coatings displayed high killing efficacies (>99.8%), were nontoxic toward mammalian fibroblasts, and demonstrated long-term stability; antimicrobial properties were retained even after 100 cleaning cycles.

While previously discussed examples were demonstrated to be highly effective against fouling, a severe downside of metallic composite-based fouling-degrading coatings is their loss of activity over time due to slow release of the biocidal component. Furthermore, metallic (nano)particles can be toxic to nontargeted organisms as well, such as natural microbes and aquatic organisms.<sup>[180,183]</sup> To avoid bioaccumulation, leaching of heavy metal-based components should be minimized in existing technologies, while extensive toxicity assays are required for new systems before they can be implemented in antifouling coatings.

### 5.3. Enzyme-Containing Coatings

A method toward fouling-degrading coatings with a lower environmental impact involves the use of enzymes. The field is already more than 30 years old, and includes applications in both medical and marine industry.<sup>[184–186]</sup> The mode of operation of such agent-releasing enzymatic coatings can be divided into direct and indirect antifouling. In a direct antifouling coating, the enzyme interferes with foulant attachment and growth itself (e.g., proteases and glycosylases), while in an indirect approach the enzyme catalyzes the formation of a biocidal component. For both approaches, the matrix can be either soluble (i.e., a self-polishing coating) or insoluble. Soluble matrices provide more stable release of the enzyme, while insoluble matrices become less effective in time due to the formation of a thick enzyme-depleted top layer that will hinder further diffusion of enzymes.<sup>[184]</sup>

The design process of an enzymatic fouling-degrading coating is plagued by several obstacles. First of all, enzyme activity typically increases with the temperature, but the stability displays an inverted relationship. Furthermore, enzymes need sufficient mobility to become catalytically active. Higher mobilities are, however, accompanied by weaker binding to the matrix, which does not guarantee long-term efficiency of the antifouling coating. Additionally, the enzyme should retain its activity when mixed with other components, but it should not affect the mechanical properties of the coating. Finally, the effectiveness of enzymes is very species-specific, which would make the combination of enzymes using different modes of operation most promising for combating biofouling.<sup>[186,187]</sup>

A recent example that involves a multicomponent indirect system was demonstrated by Wu et al.<sup>[188]</sup> Cooperation between two different enzymes, glucose oxidase and horseradish peroxidase, resulted in hydrogel formation through polymerization of a phenolic monomer and simultaneously provided antibacterial properties to the gel: bacteria were killed with high efficiency within a day (>99.99%). Multifunctional fouling-degrading coatings can also be produced by combining different types of bactericidal agents. Park et al. decorated electrospun poly(vinyl alcohol)/PAA nanofibers with proteases and Cu(II) ions: the enzymes were able to directly degrade the extracellular matrix, while the Cu(II) ions killed both bacteria and planktonic cells.<sup>[189]</sup> Such dual-action fibers could be interesting for the preparation of antimicrobial fabrics. Other interesting work was reported by Yeon et al., who presented a biocompatible approach by immobilizing glucose oxidase on magnetic chitosan-based nanoparticles.<sup>[190]</sup> The generated hydrogen peroxide (H<sub>2</sub>O<sub>2</sub>) effectively inhibited growth of bacteria in suspensions and films.

Because natural enzymatic systems are relatively unstable and very sensitive to changes in the environment, researchers have also tried to mimic enzymatic functionality using synthetic materials. Such systems are easier to synthesize, facilitate optimization, are more stable, and allow massproduction.<sup>[191]</sup> Artificial enzymes (or nanozymes) frequently involve nanoparticles with high catalytic activities, which is related to their high surface-to-volume ratio. Several mimics have been reported, such as peroxidases, oxidases, catalases and hydrolases.<sup>[192]</sup> Cerium(IV)-

containing metal-organic framework (MOF) nanozymes were for example introduced by Liu et al.<sup>[193]</sup> These particles revealed dual enzyme-mimetic activities: the Ce(IV) complex was able to hydrolyze extracellular DNA and therefore helped to degrade attached biofilms (direct desoxyribonuclease-like), while the MOF could convert H<sub>2</sub>O<sub>2</sub> into hydroxide radicals which possess high bactericidal properties (indirect peroxidase-like). Although the authors only treated fouled surfaces with dispersions of the hybrids, their nontoxicity and stability under various conditions demonstrated future potential. Herget et al. went a step further and incorporated CeO<sub>2-x</sub> nanorod-based artificial enzymes in indirect fouling-degrading coatings (Figure 7c).<sup>[170]</sup> Such particles mimic the activity of haloperoxidases, and are able to catalyze the oxidation of halides in the presence of H<sub>2</sub>O<sub>2</sub> to form the corresponding hypophalous acid. This species in turn is reactive toward the signaling molecules of bacteria, and will thereby hinder intercellular communication. The synthesized CeO<sub>2-x</sub> nanorods were subsequently introduced in both hard and soft (i.e., self-polishing) paint formulations. Compared to a commercial cuprous oxide-based coating, both nanozyme coatings performed better in lab tests (Gram-negative bacteria) and field tests (algae biofouling), even at lower concentrations, and demonstrated lower toxicities. The same material was later also successfully implemented in electrospun polymer fabrics that may be promising for use in tissue engineering, wearable electronics and water purification (Figure 7d).<sup>[171]</sup>

Although nanozymes do tackle some of the problems that are encountered in natural enzymatic coatings, these novel nanoparticle-based systems are likely plagued by the same issues as the metallic (nano)composites (see Section 5.2): their ecotoxicological impact should be assessed before they can be implemented in commercial fouling-degrading coatings.

### 5.4. Photoactive Coatings

Photoactive coatings only exhibit fouling-degrading properties upon irradiation by light. During such an event, the photosensitizer absorbs light, transfers energy to molecular oxygen or water to generate highly toxic ROS.<sup>[194]</sup>

Due to their high UV-induced photocatalytic activity, titanium dioxide-containing materials are among the most studied photoactive coatings.<sup>[195]</sup> Wei et al. improved the fouling-degrading performance of Cu(0)/epoxy composite resins by incorporating TiO<sub>2</sub> nanoparticles.<sup>[196]</sup> Addition of only 1 wt% TiO<sub>2</sub> already led to a significant enhancement of the antibacterial properties; full elimination of *E. coli* bacteria could be accomplished within 2 h under sunlight. Furthermore, TiO<sub>2</sub> increased the mechanical properties of the epoxy coating, and this method allowed facile modification of several substrates, such as glass, wood and steel. Chambers et al. studied the effect of silver-doping of TiO<sub>2</sub> nanoparticles; Ag doping levels of up to 8% caused the absorption band to shift from UV to the blue region of the visible spectrum.<sup>[197]</sup> Photoactive epoxy-based composite resins demonstrated complete killing of bacteria when exposed to visible light.

The high surface energy of TiO<sub>2</sub>, however, often causes particle aggregation to occur in such photoactive composites. As a consequence, recombination is favored over charge transfer, and thus leads to reduced ROS formation. By either including

graphene oxide<sup>[198]</sup> or covering the nanoparticles with a layer of graphene,<sup>[199]</sup> increased photocatalytic activity was demonstrated due to 1) inhibition of particle aggregation and 2) more efficient energy transfer to water or oxygen via the carbon component. Moreover, smoother surfaces were formed in case of a PVDF/graphene oxide composite, which may reduce fouling in the absence of light as well.

Besides TiO<sub>2</sub>, other metal oxides have been reported to display photocatalytic activity. These include AgCl/ZnO nanocomposites and their incorporation in biocompatible chitosan hydrogels,<sup>[200]</sup> and nontoxic SnO<sub>2</sub> microplates for the preparation of self-cleaning surfaces.<sup>[201]</sup>

The active component of photoactive fouling-degrading coatings is, however, not limited to metallic systems. Conjugated organic materials have started to attract increasing attention, because these materials allow facile optimization of the optical properties, can be processed from solution, show low toxicities, and can be easily integrated in existing polymeric coatings.<sup>[202]</sup> Porphyrins (i.e., heterocyclic macrocycles that are abundantly present in nature), are able to produce ROS as well. Their absorption wavelengths and quantum yields are tunable through side-group modification and/or metal complexation.<sup>[203]</sup> Chen et al. decorated a copolymer with porphyrin groups via host-guest interactions, and complexation to Sn(IV) ensured that the operating wavelength was shifted to the visible region (Figure 7e).<sup>[172]</sup> This supramolecular photodynamic polymer could be used to remove biofilms, and was demonstrated to be nontoxic toward mammalian cells. Heredia et al. applied a slightly different approach: Zn(II) porphyrins were functionalized with additional conjugated side groups.<sup>[204]</sup> Electropolymerization of these porphyrin-containing monomers resulted in photoactive polymeric films that produced singlet oxygen under blue light illumination. Coatings were tested against individual and biofilm-embedded microorganisms: close to 100% bacterial killing was achieved within half an hour. The only drawback of this strategy is the requirement of an electrically conductive substrate in order to form the coating itself.

A final interesting development was reported by Pan and colleagues, who coated glass-fiber membranes with polypyrrole via vapor polymerization.<sup>[205]</sup> Instead of forming ROS, these coatings produced significant amounts of heat when illuminated by sunlight. Temperatures of up to 130 °C could be reached within a minute, which enabled full removal of *E. coli* bacteria. The coatings were stable for several cycles, and may suffer less photocatalytic degradation (“chalking effect”) compared to ROS-forming systems. Furthermore, application through vapor deposition could facilitate translation to other substrates.

A significant advantage of photoactive coatings is the absence of toxicants leaching into the environment. However, their application is limited to surfaces that have easy access to light. Furthermore, thick layers of fouling material will not allow the light to pass through, meaning that frequent cleaning is required in order to preserve the photoactive degrading properties.

## 6. Combined Strategies

Fouling-resistant, fouling-release, and fouling-degrading coatings are important strategies in order to repel, release or kill

foulants. While such coatings can significantly reduce the rate of fouling, it is inevitable in the long run. Fouling-resistant coatings cannot repel each and every surface-active species existing in its operating environment.<sup>[206]</sup> Fouling-release coatings are unstable and will degrade over time, which may promote bacterial attachment instead.<sup>[20]</sup> Fouling-degrading coatings slowly lose their catalytic and/or antimicrobial activity due to depletion of the active species, and the surface may become contaminated by adhered dead bacteria. In addition, it may also kill other (untargeted) organisms, leading to environmental pollution.<sup>[20,91,169,207,208]</sup> Hence, there is a need for the development of synergistic coatings: coatings that exhibit a combination of above strategies, either consistently or when triggered, in order to guarantee an improved and long-term resistance.<sup>[206]</sup>

### 6.1. Synergistic Coatings

#### 6.1.1. Fouling-Resistant and Fouling-Release Coatings

As was described in Section 4.1, amphiphilic surfaces often display both fouling-resistant and fouling-release characteristics. Hence, a synergistic fouling-resistant and -release coating can be obtained by combining a fouling-resistant component (e.g., PEG), with a fouling-release component (e.g., fluoropolymer), into an amphiphilic coating. This way, the hydration barrier and steric repulsion of the long hydrophilic PEG chains will prevent foulant attachment, while the low surface energy of the hydrophobic fluoro chains promote rapid foulant release in case they do attach.<sup>[100,209]</sup> Several groups have developed such coatings. Xu et al. spin-coated a layer of the asymmetric molecular brush poly(perfluoromethacrylate-*b*-ethylene glycol) (PFMA-*b*-PEG) on either ITO or Si/SiO<sub>2</sub> (Figure 8a). Protein adsorption was decreased with 45% to 75%, and the cell adhesion was reduced by 70–90%.<sup>[209]</sup> Similarly, Yi et al. fabricated an amphiphilic copolymer surface by spin-coating PMMA-*g*-(PEG, PMTFPS) on a silicon wafer. In each case, the antifouling performance was very composition-dependent, as longer fluoro side chains would increase the fouling-release performance, but decrease the protein resistance, and vice versa. Therefore, a standard PEG brush would still be superior.<sup>[100]</sup> A final example includes coatings based on amphiphilic Janus particles, as was reported by the Synytska group (Figure 8b). The Janus particles were constructed by functionalizing one side of a silica particle with hydrophobic PDMS, while grafting the opposite side with hydrophilic poly(poly(ethylene glycol) methyl ether methacrylate) (PPEG-MEMA). By treating silicon wafers with this particle formulation, heterogeneous microstructured surfaces were obtained. When investigating the resistance toward bacterial adhesion, the amphiphilic Janus particle coatings outperformed the purely hydrophobic particle surfaces and the flat control samples.<sup>[210]</sup>

#### 6.1.2. Fouling-Resistant and Fouling-Degrading Coatings

Another synergistic coating involves the combination of fouling-resistant and fouling-degrading properties. Such a kill and release strategy enables a surface to kill bacteria in case they attach, after which the dead bacteria and debris are



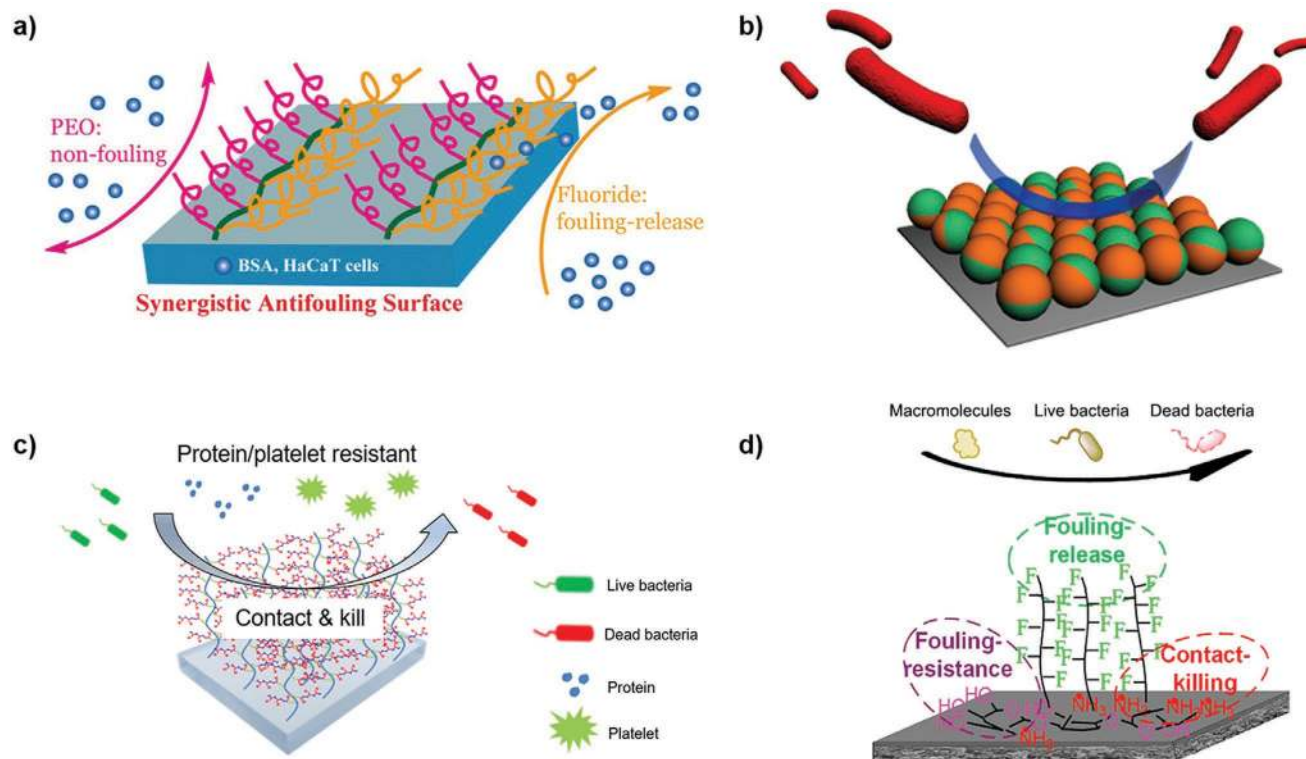


**Figure 8.** Schematic representations of synergistic antifouling (bottle) brush coatings, including a) fouling-resistant and fouling-release PFMA-*b*-PEG copolymer, b) PDMS-PPEGMEMA Janus particles, c) fouling-degrading and fouling-release graft copolymer PEG-*b*-AMP, and d) a mix of all three antifouling strategies incorporated in the TOB-fluoropolymer brushes. (a) Reproduced with permission.<sup>[209]</sup> Copyright 2017, American Chemical Society. (b) Reproduced with permission.<sup>[210]</sup> Copyright 2016, American Chemical Society. (c) Adapted with permission.<sup>[207]</sup> Copyright 2017, Elsevier. (d) Reproduced with permission.<sup>[211]</sup> Copyright 2018, Elsevier.

released by action of the fouling resisting groups, thereby maintaining long-term antifouling surface activity.<sup>[208]</sup> Goa et al. developed bottlebrush coatings of amphiphilic copolymers, containing cationic antimicrobial polypeptides (AMP) and antifouling PEG segments, grafted to the surface via a methacrylate anchor (Figure 8c). The AMP units provided the biocidal activity by interacting with and disrupting bacteria cell membranes, while the PEG chains reduced protein/platelet adhesion, prevented dead bacterial remnants from attaching to the surface and reduced the cytotoxicity of AMP. Even though standard PEG coatings still showed better protein resistance, they were not able to kill any bacteria.<sup>[207]</sup>

### 6.1.3. Fouling-Resistant, Fouling-Release, and Fouling-Degrading Coatings

Wang et al. even managed to endow membranes with anti-adhesion, self-cleaning, and antimicrobial characteristics (Figure 8d). They modified polysulfone membrane surfaces by grafting them with low surface energy fluoropolymer brushes (fouling-release), combined with hydrophilic and bactericidal tobramycin (TOB) segments (fouling-resistant, fouling-degrading). Due to the synergistic effect of TOB and the fluoropolymer brushes, foulants could be resisted and, if necessary, released from the membrane surface. In addition,

the modified surface exhibited potent antimicrobial activity with a mortality rate higher than 99.8%. This triple antifouling strategy exhibited the best antifouling properties, and clearly outperformed both the pristine and modified membranes exhibiting only one or two antifouling strategies.<sup>[211]</sup>

## 6.2. Stimuli-Responsive Coatings

Stimuli-responsive coatings can switch their interfacial properties rapidly and reversibly, according to small changes in the environment, such as temperature or pH.<sup>[12,169]</sup> Such stimuli-responsiveness, combined with antifouling properties, could turn out to be a valuable strategy toward surface regeneration. This way, in case fouling does happen, a simple trigger (e.g., salt, pH, temperature, solvent) enables easy removal of foulants and recovers the antifouling properties.

### 6.2.1. Temperature-Responsive Coatings

Coatings that involve the thermoresponsive polymer poly(*N*-isopropylacrylamide) (PNIPAAm) are able to combine fouling-resistant and fouling-degrading characteristics. PNIPAAm undergoes a sharp reversible phase transition from a soluble, swollen, hydrated and protein-repelling state at room

temperature, to an insoluble, collapsed, dehydrated and protein-adhesive conformation above its lower critical solution temperature (LCST, 32 °C).<sup>[12,169,208,215,216]</sup> The antifouling behavior below its LCST is caused by the hydration of the acrylamide groups along the polymer brush backbone.<sup>[12,216]</sup> Above the LCST, small hydrophobic pockets form between the collapsed chains, leading to irreversible adsorption of smaller proteins.<sup>[215]</sup> Yu et al. took advantage of the thermoresponsive conformational change of PNIPAAm to develop a multifunctional material that is capable of attaching, killing and releasing bacteria in a controllable manner. A biocidal quaternary ammonium salt (QAS) was incorporated into the nanopatterned regions between surface-tethered PNIPAAm brushes (**Figure 9a**). Above the lower critical solution temperature (LCST) of PNIPAAm, the collapsed polymer chains facilitated the attachment of bacteria and simultaneously exposed QAS moieties that killed attached bacteria. Upon reducing the temperature below the LCST, hydration and swelling of the PNIPAAm chains promoted the release of dead bacteria ( $\approx 67\%$ ). Hence, the kill and release strategy can also be achieved through a simple trigger, such as a change in temperature.<sup>[169]</sup>

While Yu et al. were able to switch the PNIPAAm coating from a bactericidal into a bacterial-resistant coating by decreasing the temperature, this is contrary to the requirements for medical devices. These actually need to be bactericidal at room temperature, but biorepellent under physiological con-

ditions. Hence, Wang et al. developed a hierarchical polymer architecture, consisting of a thermoresponsive poly(*N*-isopropylacrylamide-*co*-2-carboxyethyl acrylate) P(NIPAAm-*co*-CEA) upper layer, grafted on top of an antifouling poly(sulfobetaine methacrylate) (PSBMA) bottom layer (**Figure 9b**). In addition, glycopeptide antibiotic vancomycin (Van) groups were covalently attached to the P(NIPAAm-*co*-CEA) brushes. At room temperature ( $<LCST$ ), the PNIPAAm-based upper layer was stretched out into solution, facilitating contact killing of bacteria by Van (88.6%). At physiological temperatures ( $>LCST$ ), the dehydrated PNIPAAm-based layer collapsed, leading to the burial of Van groups and disruption of the hydrogen bonds between Van and bacteria. Furthermore, the exposed hydrophilic PSBMA brushes further facilitated the detachment of dead bacteria and suppressed additional bacterial adhesion.<sup>[208]</sup>

### 6.2.2. pH-Responsive Coatings

Besides a temperature trigger, a pH trigger can also cause a coating to switch from fouling-resistant to fouling-degrading, and vice versa. Weinman and co-workers investigated the biofouling minimization of ultrafiltration polyethersulfone membranes by grafting them with the carboxybetaine zwitterionic polymer poly(2-((2-hydroxy-3-(methacryloyloxy)propyl)

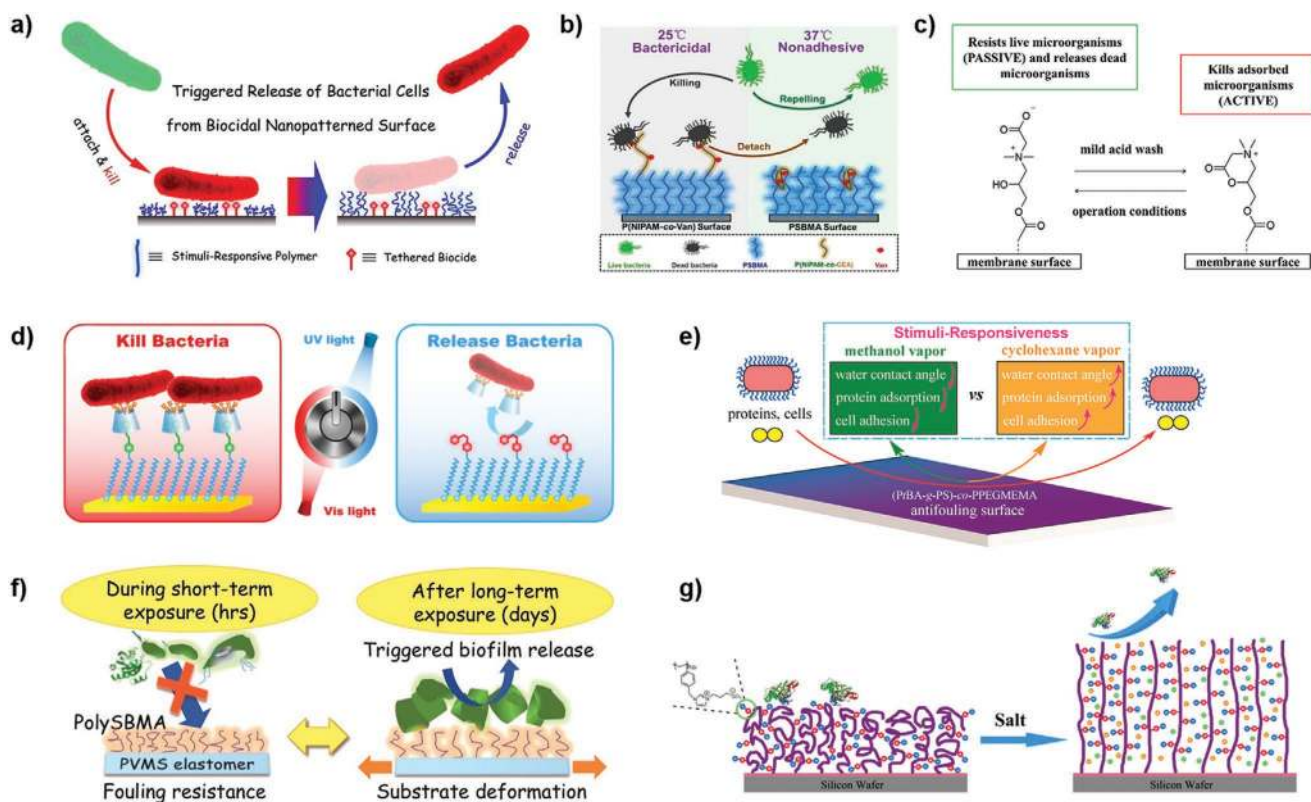


**Figure 9.** Schematic representation of stimuli-responsive antifouling coatings, including a) thermoresponsive PNIPAAm-QAS and b) PNIPAAm-Van, c) pH-responsive polyCBOH, d) light-responsive Azo/CD-QAS, e) solvent-responsive (PBA-*g*-PS)-*co*-PPEGMEMA, f) strain-responsive PVMS-PSBMA, and g) salt-responsive polyVBIPS. (a) Reproduced with permission.<sup>[169]</sup> Copyright 2013, American Chemical Society. (b) Reproduced with permission.<sup>[208]</sup> Copyright 2017, American Chemical Society. (c) Reproduced with permission.<sup>[21]</sup> Copyright 2017, Elsevier. (d) Reproduced with permission.<sup>[212]</sup> Copyright 2017, American Chemical Society. (e) Reproduced with permission.<sup>[213]</sup> Copyright 2016, ACS American Chemical Society. (f) Reproduced with permission.<sup>[206]</sup> Copyright 2015, American Chemical Society. (g) Adapted with permission.<sup>[214]</sup> Copyright 2015, American Chemical Society.

dimethylammonio)acetate (poly(CBOH)) (Figure 9c). When decreasing the solution pH to a value of 1.0, the polymer switched from a linear zwitterionic state (poly(CBOH)) to a cyclic cationic state (poly(CB-Ring)) within 15 min. As a consequence, the fouling-resistant activity of the coating changed into an antimicrobial ability. The quaternary amine disrupted the cell membrane of bacteria, resulting in cell leakage and eventually cell death. The poly(CB-Ring) switched back to poly(CBOH) when exposed to normal operating conditions (pH > 1.0). The coating could withstand many switching cycles (at least 50).<sup>[21]</sup>

### 6.2.3. Light-Responsive Coatings

While pH and temperature are very attractive triggers, it may be limiting for use in biomedical applications. Instead, light is non-invasive and intrinsically clean in nature, and can also trigger a coating to reversibly switch from fouling-degrading to fouling-releasing. Wei et al. developed such a smart and light-responsive supramolecular kill and release antibacterial surface (Figure 9d). The surface was covered with an azobenzene (Azo)-containing SAM and biocidal  $\beta$ -cyclodextrin ( $\beta$ -CD), decorated with seven QAS groups (CD-QAS). In the trans-form, the Azo groups can form reversible inclusion complexes with CD-QAS moieties via host-guest interactions, resulting in a strongly bactericidal surface that kills >90% of the attached bacteria. On irradiation with UV light, the photoresponsive Azo groups switch to the bent cis form and no longer fit inside the  $\beta$ -CD cavity, resulting in the dissociation of the Azo/CD-QAS inclusion complex and release of dead bacteria from the surface (>95%). Bacteria can also be released by introducing a competitive guest molecule with a higher affinity for  $\beta$ -CD, like adamantane. After this kill and release cycle, the surface could be easily regenerated for reuse by irradiation with visible light and reincorporation of fresh CD-QAS.<sup>[212]</sup>

### 6.2.4. Solvent-Responsive Coatings

A change of solvent can trigger the coating to switch from fouling-resistant to fouling-releasing. Xu et al. prepared amphiphilic polymer brush thin films by spin-casting a solution of asymmetric (PtBA-g-PS)-co-PPEGMEMA copolymer onto a surface (Figure 9e). The hydrophilic PEG side chains formed brush-like structures that prevented proteins from penetrating to the substrate surface, while the hydrophobic PS side chains with low interfacial surface energies showed good fouling-release properties. Exposure to methanol resulted in swelling and concurrent enrichment of PEG chains at the film surface, which increased the hydrophilicity and the resistance to protein and cell adhesion. When the film was exposed to a more hydrophobic solvent, such as cyclohexanone, the surface became enriched with PS chains, which increased the hydrophobicity and enabled fouling-release.<sup>[213]</sup>

### 6.2.5. Strain-Responsive Coatings

Shivapooja et al. combined the superior fouling-resistant characteristics of zwitterionic PSBMA with the nontoxic and

fouling-release characteristics of poly(vinylmethyl siloxane) (PVMS) elastomer (Figure 9f). In case of an insufficient fouling-resistant performance of the zwitterionic PSBMA, foulant detachment could be triggered through surface deformation. This could be achieved either directly by stretching the PVMS elastomer substrate, or by indirect electro- and pneumatic action methods. At strains of  $\epsilon > 15\%$ , more than 85% of the biofouling was released, and could be easily removed upon gentle rinsing.<sup>[206]</sup>

### 6.2.6. Salt-Responsive Coatings

Another fouling-resistant and -release approach was developed by Chen and co-workers, who grafted a salt-responsive brush of zwitterionic poly(3-(1-(4-vinylbenzyl)-1H-imidazol-3-ium-3-yl) propane-1-sulfonate) (polyVBIPS) onto a gold surface, which was able to switch reversibly and repeatedly between protein capture/release and surface wettability in a controllable manner (Figure 9g). At low ionic strengths, the polyVBIPS brushes adopted a collapsed chain conformation, achieving a biomolecule-adhesive state: the adsorption of proteins was as high as 900 ng cm<sup>-2</sup>. Once reaching higher ionic strengths (1 M NaCl), the chains extended and a biomolecule-resistant state was obtained. This behavior was attributed to the combined effect of enhanced surface hydration and electrostatic screening by counterions (i.e., the anti-polyelectrolyte effect). Protein adsorption was reduced to 100 ng cm<sup>-2</sup> and even to <0.3 ng cm<sup>-2</sup> after washing. Hence, the introduction of salt led to protein desorption from the polyVBIPS brushes.<sup>[214,217]</sup>

Finally, Zhang et al. integrated all aforementioned anti-fouling strategies into a single hydrogel, to realize resistance, release, and killing of bacteria. They combined conjugated salt-responsive, fouling-releasing poly(3-(dimethyl(4-vinylbenzyl)ammonio)propyl sulfonate) (polyDVBAPS) with fouling-resistant poly(*N*-hydroxyethyl acrylamide) (polyHEAA) and antimicrobial Ag NPs. To this end, polyDVBAPS-g-polyHEAA@AgNPs hydrogels exhibited a strong antifouling capacity (<10<sup>6</sup> cells cm<sup>-2</sup>) up to 4 days, high antibacterial activity by killing  $\approx 99\%$  of adherent bacteria, and efficient bacterial release ( $\approx 98\%$ ) to regenerate the surface and keep it free from (dead) bacteria. By reloading the hydrogel with fresh Ag NPs after each cycle, the surface could retain its bactericidal activity.<sup>[218]</sup>

## 7. Practical Feasibility

In the previous sections, various concepts to protect surfaces from becoming fouled were introduced, but there are still many challenges to be overcome before they can be put into practice. First of all, while many of these coated surfaces show excellent antifouling properties, preserving their properties is almost impossible. In time, fouling agents with different surface characteristics or heterogeneities will adsorb from the surroundings. Secondly, degradation, accidental scratching, or other types of mechanical damage will eventually harm the anti-fouling coating and expose the underlying substrate, once again



risking contamination. Thirdly, translating the often covalently grafted and substrate-specific lab-scale antifouling coatings to a large surface area turns out to be far too difficult and expensive. Thus, we are in need of mechanically stable and durable antifouling coatings, which can be cheaply synthesized and universally applied onto large surfaces, while preserving their antifouling performance on a long-term basis. Each of these challenges will be described below, and possible solutions are proposed.

## 7.1. Mechanical Stability

Covalently attached antifouling coatings have a restricted mobility and are very difficult to repair upon mechanical damage or wear. Reinforcement strategies can help stabilize antifouling coatings. It often involves the combination of existing antifouling coatings with mechanically resistant materials (e.g., epoxy or PTU resins) and/or by incorporation of organic fillers, such as ZnO or TiO<sub>2</sub> nanoparticles (see Section 4.4).<sup>[146,219,220]</sup> In recent years, various innovative and interesting concepts have been described. Endowing the antifouling films with healable capabilities can enhance the lifetime and reliability, even when used in harsh environments.<sup>[91,221,222]</sup> Covalent or noncovalent crosslinking of antifouling films presents another way of increasing the mechanical robustness. Catch bonds are a theoretical example of noncovalent crosslinking, which actually become stronger when subjected to a mechanical force.<sup>[223]</sup> Both strategies are explained in further detail in the next sections.

### 7.1.1. Self-Healing Antifouling Coatings

One way to retain or restore antifouling properties after mechanical damage is by introducing a self-healing ability. Several kinds of self-healing coatings have been reported, including brushes, hydrogels, microspheres, nanocomposites, and polymer network films. Healing can, for example, be stimulated by heat or by the action of water.

*Heat-Enabled Healing:* One approach to induce healing after damage is via a simple heat treatment. When heated above a critical temperature, such as the glass transition temperature, the mobility of the polymer chains increases tremendously. This allows rearrangement and reformation of broken interactions in order to recover the optimal surface for antifouling.<sup>[224]</sup> Wang et al. incorporated this valuable feature in their smooth poly(2-perfluorooctylethyl methacrylate) (PMAF17) brushes. When damaged, the antifouling performance could be restored by heating the coating above its glass transition temperature of 40 °C (Figure 10a).<sup>[224]</sup> The increased temperature induced the movement of undamaged fluorinated tails to the surface, thereby repairing the fractured coating. Moreover, nanostructured PMAF17 brushes enhanced the antifouling performance and self-healing rate even further (Figure 10b). The latter was attributed to the increased interbrush spacing on the nanostructured surface, which allowed the brush segments to more readily orient themselves

during the heat treatment, resulting in faster self-healing.<sup>[225]</sup> Whereas the damaged brush hidden below the repaired top-layer will not influence the surface characteristics initially, it may still affect the layer structure. Hence, after increased and repeated damage, the polymer reorientation processes will be insufficient, and consequently more permanent damage will result.<sup>[224]</sup>

*Water-Enabled Healing:* Another approach toward self-healing is by the action of water. Addition of water leads to swelling which can partially seal scratches, but it also increases the mobility of the chains near the fractured surfaces, enabling reformation of supramolecular interactions, resulting in complete healing.<sup>[222,226]</sup> This type of self-healing was implemented in the zwitterionic polymer network of Wang et al. by copolymerizing antifouling and zwitterionic 2-[(methacryloyloxy)ethyl] dimethyl-(3-sulfopropyl) ammonium hydroxide (MEDSAH) with the antifouling crosslinker poly(ethylene glycol) dimethacrylate (Figure 10c). In case of damage, the foulants would accumulate inside the scratch. Immersion in water fully recovered both mechanical and antifouling properties within a minute due to reformation of electrostatic interactions (Figure 10d).<sup>[226]</sup> Chen et al. showed that the LbL assembly of PEGylated branched PEI (bPEI) and HA, followed by PEG diacid crosslinking, also resulted in highly effective, and substrate-independent, water-healable antifouling films.<sup>[222]</sup>

Unfortunately, the above-mentioned coatings have their limitations: once the dimensions of a scratch become larger than a certain critical size, the self-healing process cannot be completed. A possible solution to this problem involves poly(ethyl acrylate)-*b*-PMEDSAH core shell microspheres, drop-casted on silicon nitride (Figure 10e). This coating can heal both nano/micro scratches and macro damage, due to the perfect balance between flexibility and structural strength; it allows for molecular mobility, but at the same time it can withstand substantial abrasion and surface restructuring.<sup>[227]</sup>

### 7.1.2. Catch Bonds

An unexplored approach to increase mechanical stability, which may display self-healing characteristics as well, involves noncovalent catch bonds. In contrast to the conventional “slip bonds”, whose lifetimes decrease with force, catch bonds actually become stronger under mechanical deformation (Figure 11a). In addition, their noncovalent character allows facile reformation in case rupture does occur, resulting in rapid strain recovery and preventing irreversible structural damage. Hence, in theory, catch bonds could both resist and recover from mechanical deformation.<sup>[223,228,229]</sup> On a conceptual level, the mechanical behavior of catch bonds can be compared to the finger trap toy, or when pulling your finger out of non-Newtonian “oobleck” (cornstarch in water): the harder you pull, the more tightly your fingers become stuck inside.<sup>[223]</sup>

Unfortunately, while catch bonds are present in a number of biological systems, it is still too complex to be experimentally demonstrated in synthetic materials. Theoretically, it has been shown that they could be utilized for building synthetic ligand-binding constructions, but also for enhancing the mechanical

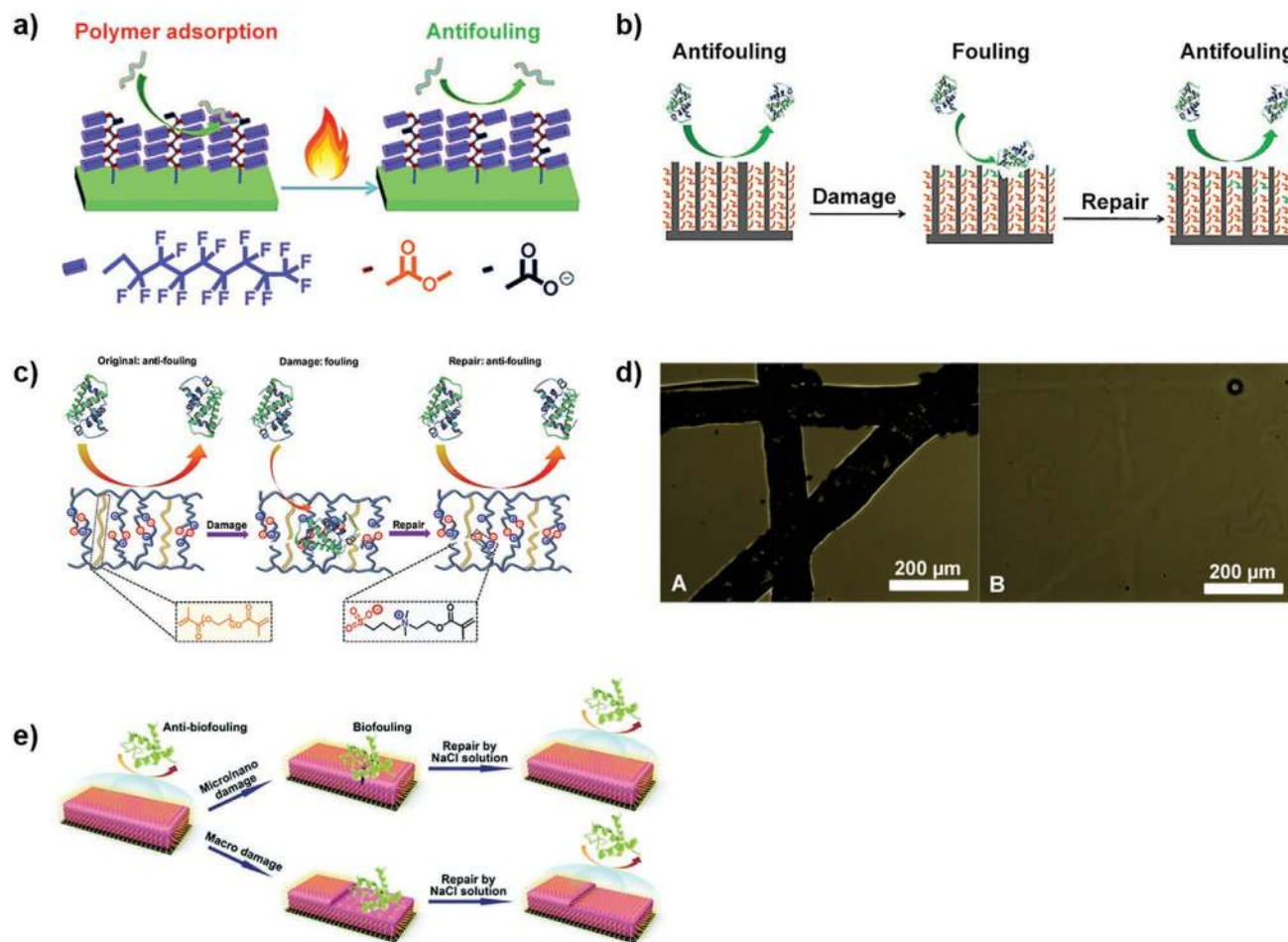


**Figure 10.** Schematic representations of antifouling coatings with heat-enabled self-healing properties, including a) fluoropolymer brushes on flat and b) nanostructured silicon surfaces,<sup>[224,225]</sup> a water-enabled self-healing property, including c) zwitterionic polymer networks, and e) self-assembled core-shell microspheres. d) All strategies showed both antifouling and self-healing characteristics. (a) Reproduced with permission.<sup>[224]</sup> Copyright 2016, The Royal Society of Chemistry. (b) Reproduced with permission.<sup>[225]</sup> Copyright 2016, American Chemical Society. (c,d) Reproduced with permission.<sup>[226]</sup> Copyright 2017, The Royal Society of Chemistry. (e) Reproduced with permission.<sup>[227]</sup> Copyright 2017, The Royal Society of Chemistry.

properties of polymer-grafted nanoparticle networks and complex coacervates.<sup>[228,230]</sup> In the case of complex coacervates, or other charge-driven assemblies, catch bonds could be incorporated as helix- or rigid-ring based ionic bonds (Figure 11b). Upon loading, the helices unfold and the rings deform, allowing more ionic interactions to be formed, thus strengthening the complex as a whole.<sup>[230]</sup> A successful incorporation of such mechanically resilient catch bonds within antifouling coatings could present a valuable way for improving their mechanical strength, toughness and durability.

## 7.2. Scale-Up

While many of the presented antifouling coatings are successful in keeping surfaces clean temporarily, there exists no generic method to produce them on a large scale. Other strategies may even turn out to be unfeasible, as is the case for pH- or solvent-responsive coatings. Transferring a coated ship from a saline environment to an acidic or hydrophobic environment

every month is simply impractical. Moreover, it is essential to keep the availability and costs of antifouling materials in mind when applied on a larger scale. Hence, a growing need exists for cost-effective coating strategies that enable rapid and facile surface modification on larger scales without the need for surface pretreatments or harsh reaction conditions. To achieve this goal, many scale-up challenges have to be overcome, as will be explained in the upcoming sections.<sup>[100]</sup>

### 7.2.1. Surface Modification Method

The well-known controllable covalent methods, including grafting to and grafting from, can produce high-density brushes, but suffer from serious limitations, including substrate specificity, susceptibility toward degradation, and complicated, expensive protocols.<sup>[73,231]</sup> Hence, covalent strategies are problematic to translate to larger surface areas in an easy and facile way. An attractive technique to easily and quickly coat large surfaces is via noncovalent strategies, such as simple

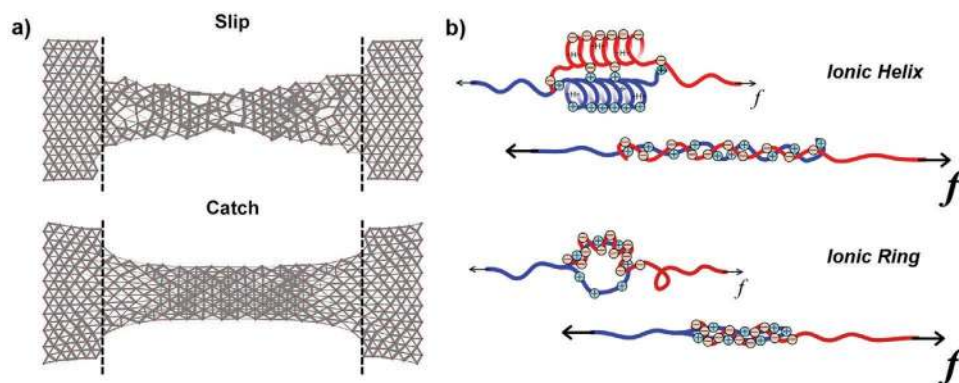


**Figure 11.** a) Schematic representations of “slip bonds” versus “catch bonds”. Adapted with permission.<sup>[223]</sup> Copyright 2015, Elsevier. b) Theoretical incorporation of catch bonds into polyelectrolyte complexes. The image was kindly provided by and used with permission from Evan Spruijt.<sup>[230]</sup>

adsorption and LbL deposition. Indeed, polymer brushes can also be generated via simple adsorption of amphiphilic block copolymers onto a selective surface (Figure 12a). However, already in an early adsorption stadium, the osmotic barrier of the initially formed brush prevents it from becoming denser, resulting in low and uncontrolled grafting densities. De Vos et al. managed to solve this problem with the zipper brush approach (Figure 12b). In their work, a water-soluble cationic/neutral diblock copolymer, quaternized poly(*N*-methyl-2-vinylpyridinium)-*b*-PEG (qp2MVP-*b*-PEG), adsorbed onto an oppositely charged PAA polyelectrolyte brush. Once full charge compensation was reached, adsorption stopped. Since the grafting density is determined by a full charge compensation rule, the grafting density of the neutral PEG brush can be controlled by adjusting the size of the qp2MVP brush with respect to the PAA chain. In addition, since the adsorbing chains do not have to fully penetrate the PAA brush in order to adsorb, higher brush densities can be achieved compared to conventional brush systems.<sup>[10,232]</sup> Thus, even with a simple adsorption method, high grafting densities can be achieved.

Contrary to the simple adsorption method, the LbL technique presents a substrate-independent method for coating large surface areas with various antifouling materials. It is carried out by alternately dipping substrates into oppositely charged polyelectrolyte solutions or by spraying these solutions onto the surface (Figure 12c). This allows a gradual and controlled built-up of antifouling PEMs.<sup>[233,234]</sup> For instance, the healable antifouling crosslinked (bPEI-PEG/HA) films of Chen et al. mentioned in Section 7.1.1 have been established by LbL assembly.<sup>[222]</sup>

While the simplicity of aforementioned noncovalent techniques makes these the most promising candidates for any large-scale application, they lack sufficient stability for usage in marine or biomedical applications. A promising strategy to improve noncovalent techniques is through their combination with a covalent crosslinking step. This way, application of the coating remains easy, but it also results in stable surface binding and sufficient mechanical strength. Yu et al. stabilized their polyglycerol-based brushes by benzophenone functionalization, which acts as both an anchor and crosslinker. Once adsorbed to the surface, the weak hydrophobic interactions between the benzophenone units and to the substrate were

further strengthened by photo-induced crosslinking (Figure 12d). The resulting crosslinked polyglycerol brushes maintained their stability and impressive antifouling performance (>95%) for at least 1 year in physiological buffer.<sup>[235]</sup>

### 7.2.2. Substrate Dependency

Another challenge that hinders upscaling involves the surface-specific conditions of many coating strategies and surface modifications known. Zwitterionic polymers for one are great antifouling alternatives to the autoxidized PEG, but their surface-specific immobilization limits their usability.<sup>[91]</sup> One way to solve this problem is to find a universal substrate that allows straightforward and diverse surface modifications. Another method involves the use of surface-independent strategies, such as the LbL method, or by incorporation of surface-independent anchoring/adhesive groups into existing antifouling coatings. Lubricin, a glycoprotein mentioned in Section 2.2, presents such an adhesive, as it self-assembles onto basically any substrate. Catechol groups (such as in polydopamine) can also self-adhere to various surfaces, as was demonstrated by Sundaram et al. Assisted by dopamine, the DOPA-functionalized carboxybetaine-based polymers (DOPA-PCB) could be attached to hydrophilic, hydrophobic and metallic surfaces in water via a simple one-step dip-coating method (Figure 12e). Since dopamine can self-polymerize, the DOPA functionality of DOPA-PCB could react with polydopamine either in solution or adsorbed on the surface, resulting in direct attachment of PCB polymer to the surface in a single step. Such dopamine-assisted DOPA-PCB coatings showed <10% fouling compared to their corresponding uncoated controls.<sup>[236]</sup>

### 7.3. Antifouling Durability

Fouling is a highly complex process, which spans numerous length and time scales, and involves a huge variety of molecules and organisms, all with their own size, shape, and composition. Due to the amphiphilic nature of foulants, coated surfaces have been proven to be insufficient to suppress fouling permanently.<sup>[1,209,213]</sup> Regardless of the antifouling methods



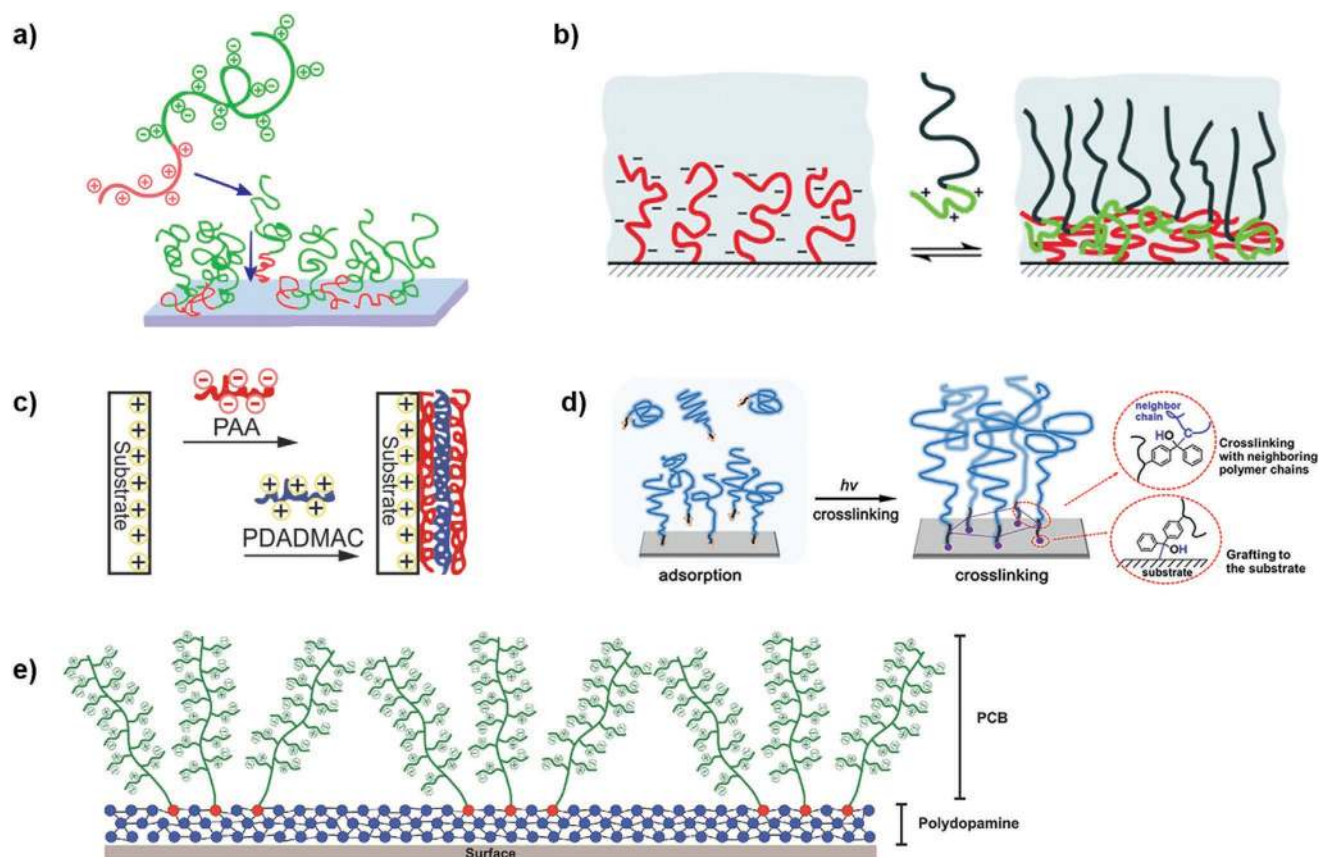


**Figure 12.** Illustrations of surface modification methods, including a) simple adsorption, b) zipper brush assembly, c) layer-by-layer deposition, and d) simple adsorption combined with benzophenone crosslinking for enhanced stabilization. e) Substrate-independent DOPA anchoring groups are one way for applying coatings universally. (a) Adapted with permission.<sup>[102]</sup> Copyright 2017, American Chemical Society. (b) Reproduced with permission.<sup>[232]</sup> Copyright 2009, Wiley-VCH. (c) Adapted with permission.<sup>[233]</sup> Copyright 2015, American Chemical Society. (d) Reproduced with permission.<sup>[235]</sup> Copyright 2017, American Chemical Society. (e) Reproduced with permission.<sup>[236]</sup> Copyright 2008, Wiley-VCH.

employed, all surfaces will eventually become fouled under adverse conditions.<sup>[237]</sup> While stimuli-responsive coatings presented a valuable way of cleaning fouled surfaces, its large-scale applicability, but also its durability, remain a big question mark. Many switching cycles may degrade the coating and reduce the antifouling performance, and foulants will start adhering again. Hence, preserving the antifouling performance on a long-term basis may be difficult. However, there are methods to regularly recover the antifouling properties. Several options are described in the following sections.

### 7.3.1. Smart Cleaning

Simple cleaning procedures are already thoroughly integrated in many antifouling techniques, mostly involving the removal of detached foulants by means of a water stream. However, other cleaning techniques can also be used to remove adhered foulants, either chemically, mechanically or optically. Such techniques include chemical treatment (e.g., surfactants, oxidizing agents), heating, sonication, scrubbing, gamma rays, air (nano) bubbles, jet spraying, pH changes and even explosives.<sup>[2,240–244]</sup> Unfortunately, most of these cleaning procedures have downsides, as they involve toxic chemicals, consume significant

amounts of energy or may damage the coating. Instead, smart cleaning strategies should be developed which act in unity with the antifouling coating, thereby ensuring a safe self-renewal process while preserving the (remaining) coating. To achieve smart cleaning methods, a cleaning capability should already be incorporated in the design of the antifouling coating itself. One could think of designing a surfactant-responsive antifouling coating, which can drastically swell or shrink in response to the addition of surfactant, thereby releasing foulant particles.<sup>[245]</sup> Another possibility is the incorporation of biodegradable groups inside the antifouling coating. The self-crosslinked and protein-resistant 3D antifouling network of Xie et al. included biodegradable 2-methylene-1,3-dioxepane (MDO) chains. In case of extensive fouling, enzymatic degradation in the presence of lipase initiated the cleaning process. It cleaved the ester linkages within the MDO main chain, thereby releasing small fragments and fouling organisms, which could easily be washed away. Such biodegradability is also very favorable when used in marine environments, although enzyme-secreting microorganisms may degrade the polymers prematurely.<sup>[246]</sup> Instead of sequential degradation, continuous and uniform degradation has also been realized (Figure 13a). The fish skin-inspired poly[(ethylene oxide)-co-(ethylene carbonate)] brushes of Cao et al. exhibited a self-renewal property through



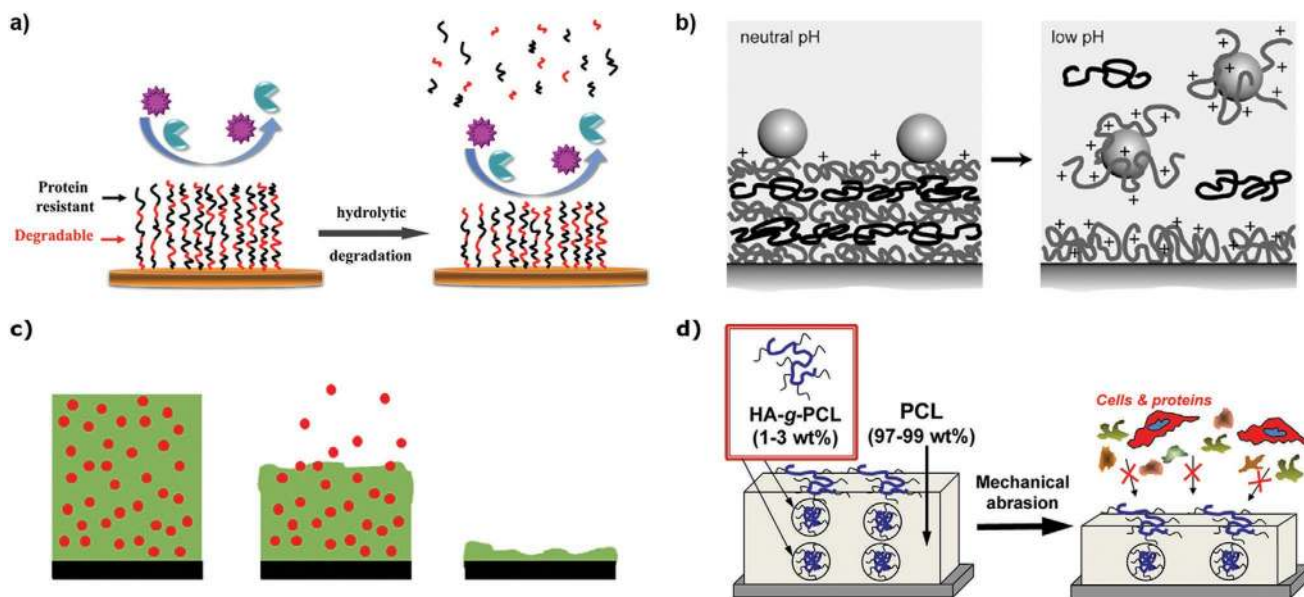


**Figure 13.** Methods to preserve the antifouling performance, either via a) smart cleaning, b) sacrificial surfaces, c) self-polishing biocidal coatings,<sup>[17]</sup> or d) nonbiocidal coatings. (a) Reproduced with permission.<sup>[238]</sup> Copyright 2019, American Chemical Society. (b) Reproduced with permission.<sup>[239]</sup> Copyright 2010, Elsevier. (c) Adapted with permission.<sup>[17]</sup> Copyright 2015, The Royal Society of Chemistry. (d) Reproduced with permission.<sup>[221]</sup> Copyright 2016, American Chemical Society.

the gradual hydrolytic cleavage of the ethylene carbonate (EC) groups in seawater, while remaining antifouling owing to the EO units. This way, adhered inorganics and organics could be polished away continuously, similar to the way fish can remove attached marine organisms from its skin by continuous mucus secretion and removal.<sup>[238]</sup>

### 7.3.2. Sacrificial Surfaces

Biological antifouling surfaces cope with damage by initiating growth and regeneration; this self-renewal property can also be integrated in synthetic antifouling materials. Stimuli-responsive coatings allow the regeneration of the antifouling performance by triggered release of foulants. Unfortunately, their cleaning efficiency never reaches 100%, and it becomes even worse after repeated cycling. Another type of regenerative coating, the sacrificial coating, not only involves the triggered release of foulants, but desorbs the complete (fouled) coating from the surface. The cleaned surface can subsequently be recoated with a new and fully functioning antifouling layer.<sup>[247]</sup> Since no direct contact between the interface and the fouling agent needs to be broken, it has the potential to remove any type of fouling material.<sup>[239]</sup>

Several systems exist that make use of such a sacrificial layer approach. One example involves the previously described PEMs. Ilyas et al. designed such a PEM coating on top of membranes, consisting of the two weak polyelectrolytes PAA and poly(allylamine hydrochloride) (Figure 13b). Treatment of the membrane with a solution of low pH and high ionic strength led to a full desorption of the PEM layer: PAA becomes uncharged at a low pH, and the high ionic strength further weakens the now unstable ionic complex, leading to disintegra-

tion of the layer. Moreover, the released polyelectrolytes act as anti-redeposition agents, preventing the released foulants from re-adsorbing before generation of a new PEM layer is completed. Recoating of the substrate led to a complete recovery of the resistance properties.<sup>[247]</sup>

### 7.3.3. Self-Polishing Coatings

When providing a synthetic coating with a built-in reservoir of antifouling or biocidal material, the material responds to surface abrasion by the release of this material where needed. Such self-polishing coatings are actually very similar to the sacrificial coatings, as they release part of their coating in order to regenerate the antifouling performance. However, instead of the triggered release of the complete coating, mechanical abrasion polishes away only the upper fouled layer. This way, the surface can be renewed several times, before recoating becomes necessary. This strategy has already been utilized for a long time on ship hulls, initiated after the major breakthrough of the tributyltin self-polishing copolymer coatings (TBT-SPC). These paints consist of an acrylic copolymer matrix, with TBT biocides bound to the polymer backbone via an ester-linkage (Figure 13c). When immersed in the sea, the carboxyl-TBT linkage is easily hydrolyzed, releasing the biocides into the water and inhibiting fouling. The shear movement of the seawater then removes the leftover (fouled) brittle polymer backbone, exposing a fresh TBT-coated surface. The main advantage of the SPC coating is that the polishing rate, and therefore the effectiveness and lifespan, can be controlled completely by manipulating the chemistry of the polymer. This has resulted in lifespans of up to 5 years.<sup>[3,248]</sup>

Once the adverse effects of TBT-based paints on the environment and aquatic life were exposed, they were banned completely. Its successor, the copper-based paints, encountered similar problems. Instead, to replace metal-based coatings, nonbiocidal self-polishing alternatives have been under investigation. One alternative involves the fouling repelling, self-polishing nanocomposite developed by Wang et al., which was obtained by blending bulk biocompatible polycaprolactone (PCL) with 1–3 wt% PCL-grafted antifouling HA nanoparticles (Figure 13d). In nonaqueous solutions, the HA-g-PCL nanoparticles adopt a reverse micelle-like structure with a PCL shell, allowing it to be mixed well with the PCL bulk material. Upon exposure to aqueous buffer, the HA-g-PCL nanoparticles flip into a regular micelle-like structure, revealing a hydrophilic shell of HA on the surface. This results in a hydrophilic, mucus-like layer on top, which prevents protein and cell adhesion. Since the nanoparticles are present throughout the bulk, mechanical abrasion exposes the fresh nanoparticles underneath, forming a new layer of hydrophilic HA coating and sustaining the surface's protein and cell resistance.<sup>[22]</sup>

The biodegradable, sacrificial, and self-polishing strategies, however, all share one main disadvantage: the surface of interest needs to be recoated, either after a triggered release, or once the coating has reached its completely polished state.

## 8. Outlook

Considering the desirable requirements altogether, it remains very challenging to realize a cost-effective, easy-applicable, and versatile protocol for the fabrication of efficient and durable antifouling coatings. No single chemistry has yet been identified as the universal antifouling strategy. In our opinion, trying to develop one universal coating strategy is an unreachable goal. Instead, one should make use of synergetic strengths by combining several antifouling strategies into one multifunctional coating. This could involve the combination of several types of chemistry (as was described in Section 6), but the combination of chemical (e.g., antifouling groups) and physical (e.g., microtopography) means is also highly promising, as was shown by the many examples existing in nature. At present, zwitterionic polymers are most promising for the development of next-generation antifouling materials, due to the simplicity of synthesis, ease of applicability, abundance of raw materials and availability of functional groups. However, it may still be necessary to develop new polymers and/or other materials to improve the antifouling performance, thereby focusing especially on long-term durability when used in both static and dynamic environments.

Apart from the surface chemistry and surface structure, novel surface modification and coating techniques need to be developed in order to successfully translate these coatings toward commercial (large-scale) applications. Every day, antifouling coatings with enhanced performances and new properties are being designed and demonstrated, but they never find their way outside the lab. To solve this problem, either the frequently used covalent grafting to and grafting from approaches need to be

simplified, or we should shift focus to physisorption techniques (e.g., layer-by-layer, spray-painting). Combining simple coating techniques with a self-replenishing antifouling character (to enhance antifouling durability) and crosslinkers or catch-bonds (to enhance mechanical stability), could result in technologically mature antifouling coatings with large-scale applicability.

All in all, a successful antifouling coating needs to tick many boxes: it should be durable, reliable, easily applicable, stable, cost-effective, eco-friendly, and substrate-independent. With the large amount of high-quality research that is being performed, we are getting closer to reaching this goal. With further research, more sophisticated designs, and an increasingly critical attitude, we genuinely believe that the ideal antifouling coating will become reality one day.

## Acknowledgements

This research received funding from the Dutch Research Council (NWO) in the framework of the ENW PPP Fund for the top sectors and from the Ministry of Economic Affairs in the framework of the “PPS-Toeslagregeling.”

## Conflict of Interest

The authors declare no conflict of interest.

## Keywords

antifouling, biomimetic materials, polymer brushes, stimuli-responsive materials, surface modification

Received: January 31, 2020

Revised: April 2, 2020

Published online:

- [1] C. M. Magin, S. P. Cooper, A. B. Brennan, *Mater. Today* **2010**, 13, 36.
- [2] G. D. Bixler, B. Bhushan, *Philos. Trans. R. Soc., A* **2012**, 370, 2381.
- [3] W. J. Yang, K. G. Neoh, E. T. Kang, S. L. M. Teo, D. Rittschof, *Prog. Polym. Sci.* **2014**, 39, 1017.
- [4] J. Rodríguez-Hernández, *Polymers Against Microorganisms*, Springer, New York **2017**.
- [5] K. A. Dafforn, J. A. Lewis, E. L. Johnston, *Mar. Pollut. Bull.* **2011**, 62, 453.
- [6] J. Fu, H. Zhang, Z. Guo, D. Qing Feng, V. Thiyagarajan, H. Yao, *J. R. Soc., Interface* **2018**, 15, 20170823.
- [7] W. L. Chen, R. Cordero, H. Tran, C. K. Ober, *Macromolecules* **2017**, 50, 4089.
- [8] S. Gon, M. M. Santore, *Langmuir* **2011**, 27, 15083.
- [9] W. M. de Vos, T. Cosgrove, J. M. Kleijn, A. de Keizer, M. A. C. Stuart, *Polymer Brushes: Kirk-Othmer Encyclopedia of Chemical Technology*, Wiley Sons Inc., Germany **2010**, p. 1.
- [10] W. M. De Vos, G. Meijer, A. De Keizer, M. A. Cohen Stuart, J. M. Kleijn, *Soft Matter* **2010**, 6, 2499.
- [11] M. Kobayashi, Y. Terayama, H. Yamaguchi, M. Terada, D. Murakami, K. Ishihara, A. Takahara, *Langmuir* **2012**, 28, 7212.
- [12] S. Burkert, E. Bittrich, M. Kuntzsch, M. Müller, K. J. Eichhorn, C. Bellmann, P. Uhlmann, M. Stamm, *Langmuir* **2010**, 26, 1786.

- [13] J. H. Lee, J. Kopecek, J. D. Andradet, *J. Biomed. Mater. Res.* **1989**, 23, 351.
- [14] M. E. Norman, P. Williams, L. Illum, *Biomaterials* **1992**, 13, 841.
- [15] S. Herrwerth, W. Eck, S. Reinhardt, M. Grunze, *J. Am. Chem. Soc.* **2003**, 125, 9359.
- [16] H. Li, V. Chen, *Membrane Technology – A Practical Guide to Membrane Technology and Applications in Food and Bioprocessing*, Butterworth-Heinemann Ltd., UK **2010**, pp. 213–254.
- [17] A. G. Nurioglu, A. C. C. Esteves, G. De With, *J. Mater. Chem. B* **2015**, 3, 6547.
- [18] H. Thérien-Aubin, L. Chen, C. K. Ober, *Polymer* **2011**, 52, 5419.
- [19] V. B. Damodaran, S. N. Murthy, *Biomater. Res.* **2016**, 20, 18.
- [20] G. P. Sakala, M. Reches, *Adv. Mater. Interfaces* **2018**, 5, 1800073.
- [21] E. Ostuni, R. G. Chapman, R. E. Holmlin, S. Takayama, G. M. Whitesides, *Langmuir* **2001**, 17, 5605.
- [22] S. Chen, L. Li, C. Zhao, J. Zheng, *Polymer* **2010**, 51, 5283.
- [23] E. P. K. Currie, W. Norde, M. A. C. Cohen Stuart, *Adv. Colloid Interface Sci.* **2003**, 100–102, 205.
- [24] A. M. Brzozowska, B. Hof, A. De Keizer, R. Fokkink, M. A. C. Stuart, W. Norde, *Colloids Surf. A Physicochem. Eng. Asp.* **2009**, 347, 146.
- [25] L. Q. Xu, K. G. Neoh, E. T. Kang, *ACS Symp. Ser.* **2018**, 1285, 233.
- [26] S. Krishnan, C. J. Weinman, C. K. Ober, *J. Mater. Chem.* **2008**, 18, 3405.
- [27] I. Banerjee, R. C. Pangule, R. S. Kane, *Adv. Mater.* **2011**, 23, 690.
- [28] L. Delauney, C. Compare, M. Lehaitre, *Ocean Sci.* **2010**, 6, 503.
- [29] J. W. Yau, H. Teoh, S. Verma, *BMC Cardiovasc. Disord.* **2015**, 15, 130.
- [30] M. Hamilos, S. Petousis, F. Parthenakis, *Cardiovasc. Diagn. Ther.* **2018**, 8, 568.
- [31] H. Yang, W. Zhang, T. Chen, S. Huang, B. Quan, M. Wang, J. Li, C. Gu, J. Wang, *Molecules* **2019**, 24, 27.
- [32] X. Cao, M. E. Pettitt, F. Wode, M. P. A. Sancet, J. Fu, J. Jian, M. E. Callow, J. A. Callow, A. Rosenhahn, M. Grunze, *Adv. Funct. Mater.* **2010**, 20, 1984.
- [33] A. V. Bers, M. Wahl, *Biofouling* **2004**, 20, 43.
- [34] M. Carve, A. Scardino, J. Shimeta, *Biofouling* **2019**, 35, 597.
- [35] B. Bhushan, Y. C. Jung, *Prog. Mater. Sci.* **2011**, 56, 1.
- [36] B. Garipcan, S. Maenz, T. Pham, U. Settmacher, K. D. Jandt, J. Zanow, J. Bossert, *Adv. Eng. Mater.* **2011**, 13, B54.
- [37] S. Gangadoo, S. Chandra, A. Power, C. Hellio, G. S. Watson, J. A. Watson, D. W. Green, J. Chapman, *J. Mater. Chem. B* **2016**, 4, 5747.
- [38] C. P. Hsu, Y. M. Lin, P. Y. Chen, *JOM* **2015**, 67, 744.
- [39] D. W. Bechert, M. Bruse, W. Hage, *Exp. Fluids* **2000**, 28, 403.
- [40] A. Gao, Y. Yan, T. Li, F. Liu, *Mater. Lett.* **2019**, 237, 240.
- [41] A. Haghdoost, R. Pitchumani, *Langmuir* **2014**, 30, 4183.
- [42] Y. Wang, W. Zhao, W. Wu, C. Wang, X. Wu, Q. Xue, *ACS Appl. Bio Mater.* **2019**, 2, 155.
- [43] K. K. Chung, J. F. Schumacher, E. M. Sampson, R. A. Burne, P. J. Antonelli, A. B. Brennan, *Biointerphases* **2007**, 2, 89.
- [44] A. M. Brzozowska, F. J. Parra-Velandia, R. Quintana, Z. Xiaoying, S. S. C. Lee, L. Chin-Sing, D. Jańczewski, S. L. M. Teo, J. G. Vancso, *Langmuir* **2014**, 30, 9165.
- [45] M. Yamamoto, N. Nishikawa, H. Mayama, Y. Nonomura, S. Yokojima, S. Nakamura, K. Uchida, *Langmuir* **2015**, 31, 7355.
- [46] S. S. Latthe, C. Terashima, K. Nakata, A. Fujishima, *Molecules* **2014**, 19, 4256.
- [47] B. Bhushan, Y. C. Jung, K. Koch, *Philos. Trans. R. Soc., A* **2009**, 367, 1631.
- [48] J. Li, E. Ueda, D. Paulssen, P. A. Levkin, *Adv. Funct. Mater.* **2019**, 29, 1.
- [49] F. Moerman, E. Partington, *Novel Materials of Construction in the Food Industry*, Elsevier Ltd, Amsterdam **2016**.
- [50] T. S. Wong, S. H. Kang, S. K. Y. Tang, E. J. Smythe, B. D. Hatton, A. Grinthal, J. Aizenberg, *Nature* **2011**, 477, 443.
- [51] S. Amini, S. Kolle, L. Petrone, O. Ahanotu, S. Sunny, C. N. Sutanto, S. Hoon, L. Cohen, J. C. Weaver, J. Aizenberg, N. Vogel, A. Miserez, *Science* **2017**, 357, 668.
- [52] Y. Wang, W. Zhao, W. Wu, C. Wang, X. Wu, Q. Xue, *ACS Appl. Bio Mater.* **2019**, 2, 155.
- [53] D. Helmer, N. Keller, F. Kotz, F. Stolz, C. Greiner, T. M. Nargang, K. Sachsenheimer, B. E. Rapp, *Sci. Rep.* **2017**, 7, 1.
- [54] N. Keller, J. Bruchmann, T. Sollich, C. Richter, R. Thelen, F. Kotz, T. Schwartz, D. Helmer, B. E. Rapp, *ACS Appl. Mater. Interfaces* **2019**, 11, 4480.
- [55] H. Zhao, Q. Sun, X. Deng, J. Cui, *Adv. Mater.* **2018**, 30, 1.
- [56] F. Dundar Arisoy, K. W. Kolewe, B. Homyak, I. S. Kurtz, J. D. Schiffman, J. J. Watkins, *ACS Appl. Mater. Interfaces* **2018**, 10, 20055.
- [57] T. W. Kim, *J. Nanosci. Nanotechnol.* **2014**, 14, 7562.
- [58] M. L. Carman, T. G. Estes, A. W. Feinberg, J. F. Schumacher, W. Wilkerson, L. H. Wilson, M. E. Callow, J. A. Callow, A. B. Brennan, *Biofouling* **2006**, 22, 11.
- [59] M. Munther, T. Palma, I. A. Angeron, S. Salari, H. Ghassemi, M. Vasefi, A. Beheshti, K. Davami, *Appl. Surf. Sci.* **2018**, 453, 166.
- [60] C. Baum, W. Meyer, R. Stelzer, L. G. Fleischer, D. Siebers, *Mar. Biol.* **2002**, 140, 653.
- [61] Z. Yang, X. Bai, X. He, C. Yuan, *ICTIS 2019 – 5th Int. Conf. Transp. Inf. Saf.* **2019**, 1192.
- [62] A. M. Brzozowska, S. Maassen, R. Goh Zhi Rong, P. I. Benke, C. S. Lim, E. M. Marzinelli, D. Jańczewski, S. L. M. Teo, G. J. Vancso, *ACS Appl. Mater. Interfaces* **2017**, 9, 17508.
- [63] A. V. Bers, E. R. Díaz, B. A. da Gama, F. Vieira-Silva, S. Dobretsov, N. Valdivia, M. Thiel, A. J. Scardino, C. D. McQuaid, H. E. Sudgen, J. C. Thomason, M. Wahl, *Biofouling* **2010**, 26, 367.
- [64] L. Bocquet, E. Lauga, *Nat. Mater.* **2011**, 10, 334.
- [65] D. Zhang, L. Li, Y. Wu, B. Zhu, H. Song, *Appl. Surf. Sci.* **2019**, 473, 493.
- [66] X. Pu, G. Li, H. Huang, *Biol. Open* **2016**, 5, 389.
- [67] G. W. Greene, L. L. Martin, R. F. Tabor, A. Michalczyk, L. M. Ackland, R. Horn, *Biomaterials* **2015**, 53, 127.
- [68] S. Chen, Z. Cao, S. Jiang, *Biomaterials* **2009**, 30, 5892.
- [69] T. Fyrner, H. Lee, A. Mangone, T. Ekblad, M. E. Pettitt, M. E. Callow, J. A. Callow, S. L. Conlan, R. Mutton, A. S. Clare, P. Konradsson, B. Liedberg, T. Ederth, *Langmuir* **2011**, 27, 15034.
- [70] B. Li, P. Jain, J. Ma, J. K. Smith, Z. Yuan, H. C. Hung, Y. He, X. Lin, K. Wu, J. Pfaendtner, S. Jiang, *Sci. Adv.* **2019**, 5, eaaw9562.
- [71] K. L. Wang, Z. H. Wu, Y. Wang, C. Y. Wang, Y. Xu, *Mar. Drugs* **2017**, 15, 1.
- [72] T. Ederth, M. Lerm, B. Orihuela, D. Rittschof, *Langmuir* **2019**, 35, 1818.
- [73] J. L. Dalsin, P. B. Messersmith, *Mater. Today* **2005**, 8, 38.
- [74] I. A. Bushnak, F. H. Labeed, R. P. Sear, J. L. Keddie, *Biofouling* **2010**, 26, 387.
- [75] B. Zappone, G. W. Greene, E. Oroudjev, G. D. Jay, J. N. Israelachvili, *Langmuir* **2008**, 24, 1495.
- [76] B. Zappone, M. Ruths, G. W. Greene, G. D. Jay, J. N. Israelachvili, *Biophys. J.* **2007**, 92, 1693.
- [77] G. D. Jay, K. A. Waller, *Matrix Biol.* **2014**, 39, 17.
- [78] G. E. Aninwene, P. N. Abadian, V. Ravi, E. N. Taylor, D. M. Hall, A. Mei, G. D. Jay, E. D. Goluch, T. J. Webster, *J. Biomed. Mater. Res., Part A* **2015**, 103, 451.
- [79] Y. Xia, V. Adibnia, R. Huang, F. Murschel, J. Faivre, G. Xie, M. Olszewski, G. De Crescenzo, W. Qi, Z. He, R. Su, K. Matyjaszewski, X. Banquy, *Angew. Chem., Int. Ed.* **2019**, 58, 1308.
- [80] O. Rendueles, J. B. Kaplan, J. Ghigo, *Environ. Microbiol.* **2013**, 15, 334.

- [81] X. Cao, M. E. Pettit, S. L. Conlan, W. Wagner, A. D. Ho, A. S. Clare, J. A. Callow, M. E. Callow, M. Grunze, A. Rosenhahn, *Biomacromolecules* **2009**, *10*, 907.
- [82] Z. Zhang, T. Chao, S. Chen, S. Jiang, *Langmuir* **2006**, *22*, 10072.
- [83] R. D. Macdonald, M. Khajehpour, *Biophys. Chem.* **2013**, *184*, 101.
- [84] E. van Andel, S. C. Lange, S. P. Pujari, E. J. Tijhaar, M. M. J. Smulders, H. F. J. Savelkoul, H. Zuilhof, *Langmuir* **2019**, *35*, 1181.
- [85] L. Zheng, H. S. Sundaram, Z. Wei, C. Li, Z. Yuan, *React. Funct. Polym.* **2017**, *118*, 51.
- [86] L. Ionov, A. Snytska, E. Kaul, S. Diez, *Biomacromolecules* **2010**, *11*, 233.
- [87] H. Ma, D. Li, X. Sheng, B. Zhao, A. Chilkoti, *Langmuir* **2006**, *22*, 3751.
- [88] X. Li, S. L. Prukop, S. L. Biswal, R. Verduzco, *Macromolecules* **2012**, *45*, 7118.
- [89] M. Divandari, G. Morgese, L. Trachsel, M. Romio, E. S. Dehghani, J. G. Rosenboom, C. Paradisi, M. Zenobi-Wong, S. N. Ramakrishna, E. M. Benetti, *Macromolecules* **2017**, *50*, 7760.
- [90] G. Morgese, L. Trachsel, M. Romio, M. Divandari, S. N. Ramakrishna, E. M. Benetti, *Angew. Chem., Int. Ed.* **2016**, *55*, 15583.
- [91] B. R. Knowles, P. Wagner, S. Maclaughlin, M. J. Higgins, P. J. Molino, *ACS Appl. Mater. Interfaces* **2017**, *9*, 18584.
- [92] C. Freij-Larsson, T. Nylander, P. Jannasch, B. Wesslén, *Biomaterials* **1996**, *17*, 2199.
- [93] N. Hui, X. Sun, S. Niu, X. Luo, *ACS Appl. Mater. Interfaces* **2017**, *9*, 2914.
- [94] K. L. Prime, G. M. Whitesides, *Science* **1991**, *252*, 1164.
- [95] K. L. Prime, G. M. Whitesides, *J. Am. Chem. Soc.* **1993**, *115*, 10714.
- [96] K. Mougín, M. B. Lawrence, E. J. Fernandez, A. C. Hillier, *Langmuir* **2004**, *20*, 4302.
- [97] T. Wazawa, Y. Ishizuka-Katsura, S. Nishikawa, A. H. Iwane, S. Aoyama, *Anal. Chem.* **2006**, *78*, 2549.
- [98] C. Wu, Y. Zhou, H. Wang, J. Hu, X. Wang, *J. Saudi Chem. Soc.* **2019**, *23*, 1080.
- [99] A. T. Nguyen, J. Baggerman, J. M. J. Paulusse, C. J. M. van Rijn, H. Zuilhof, *Langmuir* **2011**, *27*, 2587.
- [100] L. Yi, K. Xu, G. Xia, J. Li, W. Li, Y. Cai, *Appl. Surf. Sci.* **2019**, *480*, 923.
- [101] Q. Xie, J. Pan, C. Ma, G. Zhang, *Soft Matter* **2019**, *15*, 1087.
- [102] S. Kalasin, R. A. Letteri, T. Emrick, M. M. Santore, *Langmuir* **2017**, *33*, 13708.
- [103] D. Leckband, S. Sheth, A. Halperin, *J. Biomater. Sci., Polym. Ed.* **1999**, *10*, 1125.
- [104] M. Wyszogrodzka, R. Haag, *Biomacromolecules* **2009**, *10*, 1043.
- [105] R. K. Kainthan, J. Janzen, E. Levin, D. V. Devine, D. E. Brooks, *Biomacromolecules* **2006**, *7*, 703.
- [106] P. Wang, Y. Dong, S. Zhang, W. Liu, Z. Wu, H. Chen, *Colloids Surf., B* **2019**, *177*, 448.
- [107] S. Lin, B. Zhang, M. J. Skoumal, B. Ramunno, X. Li, C. Wesdemiotis, L. Liu, L. Jia, *Biomacromolecules* **2011**, *12*, 2573.
- [108] Q. Liu, A. Singh, R. Lalani, L. Liu, *Biomacromolecules* **2012**, *13*, 1086.
- [109] A. I. Lopez, A. Kumar, M. R. Planas, Y. Li, T. V. Nguyen, C. Cai, *Biomaterials* **2011**, *32*, 4336.
- [110] D. Y. Joh, F. McGuire, R. Abedini-Nassab, J. B. Andrews, R. K. Achar, Z. Zimmers, D. Mozhdzhi, R. Blair, F. Albarghouthi, W. Oles, J. Richter, C. M. Fontes, A. M. Hucknall, B. B. Yellen, A. D. Franklin, A. Chilkoti, *ACS Appl. Mater. Interfaces* **2017**, *9*, 5522.
- [111] A. Hucknall, A. J. Simnick, R. T. Hill, A. Chilkoti, A. Garcia, M. S. Johannes, R. L. Clark, S. Zauscher, B. D. Ratner, *Biointerphases* **2009**, *4*, FA50.
- [112] H. Ma, J. Hyun, P. Stiller, A. Chilkoti, *Adv. Mater.* **2004**, *16*, 338.
- [113] G. Morgese, B. Verbraeken, S. N. Ramakrishna, Y. Gombert, E. Cavalli, J. G. Rosenboom, M. Zenobi-Wong, N. D. Spencer, R. Hoogenboom, E. M. Benetti, *Angew. Chem., Int. Ed.* **2018**, *57*, 11667.
- [114] X. Zheng, C. Zhang, L. Bai, S. Liu, L. Tan, Y. Wang, *J. Mater. Chem. B* **2015**, *3*, 1921.
- [115] E. M. Benetti, M. Divandari, S. N. Ramakrishna, G. Morgese, W. Yan, L. Trachsel, *Chem. - Eur. J.* **2017**, *23*, 12433.
- [116] T. P. Galhenage, D. Hoffman, S. D. Silbert, S. J. Stafslien, J. Daniels, T. Miljkovic, J. A. Finlay, S. C. Franco, A. S. Clare, B. T. Nedved, M. G. Hadfield, D. E. Wendt, G. Waltz, L. Brewer, S. L. M. Teo, C. S. Lim, D. C. Webster, *ACS Appl. Mater. Interfaces* **2016**, *8*, 29025.
- [117] W. van Zoelen, H. G. Buss, N. C. Ellebracht, N. A. Lynd, D. A. Fischer, J. Finlay, S. Hill, M. E. Callow, J. A. Callow, E. J. Kramer, R. N. Zuckermann, R. A. Segalman, *ACS Macro Lett.* **2014**, *3*, 364.
- [118] A. L. Patterson, B. Wenning, G. Rizis, D. R. Calabrese, J. A. Finlay, S. C. Franco, R. N. Zuckermann, A. S. Clare, E. J. Kramer, C. K. Ober, R. A. Segalman, *Macromolecules* **2017**, *50*, 2656.
- [119] M. E. Barry, E. C. Davidson, C. Zhang, A. L. Patterson, B. Yu, A. K. Leonardi, N. Duzen, K. Malaviya, J. L. Clarke, J. A. Finlay, A. S. Clare, Z. Chen, C. K. Ober, R. A. Segalman, *Macromolecules* **2019**, *52*, 1287.
- [120] A. K. Leonardi, C. K. Ober, *Annu. Rev. Chem. Biomol. Eng.* **2019**, *10*, 241.
- [121] M. Lejars, A. Margaillan, C. Bressy, *Chem. Rev.* **2012**, *112*, 4347.
- [122] M. S. Selim, M. A. Shenashen, S. A. El-Safty, S. A. Higazy, M. M. Selim, H. Isago, A. Elmarakbi, *Prog. Mater. Sci.* **2017**, *87*, 1.
- [123] S. Krishnan, N. Wang, C. K. Ober, J. A. Finlay, M. E. Callow, J. A. Callow, A. Hexemer, K. E. Sohn, E. J. Kramer, D. A. Fischer, *Biomacromolecules* **2006**, *7*, 1449.
- [124] P. Majumdar, D. C. Webster, *Macromolecules* **2005**, *38*, 5857.
- [125] S. A. Sommer, J. R. Byrom, H. D. Fischer, R. B. Bodkhe, S. J. Stafslien, J. Daniels, C. Yehle, D. C. Webster, *J. Coat. Technol. Res.* **2011**, *8*, 661.
- [126] E. Martinelli, I. Del Moro, G. Galli, M. Barbaglia, C. Bibbiani, E. Mennillo, M. Oliva, C. Pretti, D. Antonioli, M. Laus, *ACS Appl. Mater. Interfaces* **2015**, *7*, 8293.
- [127] H. S. Sundaram, Y. Cho, M. D. Dimitriou, C. J. Weinman, J. A. Finlay, G. Cone, M. E. Callow, J. A. Callow, E. J. Kramer, C. K. Ober, *Biofouling* **2011**, *27*, 589.
- [128] S. Holberg, R. Losada, F. H. Blaikie, H. H. W. B. Hansen, S. Soreau, R. C. A. Onderwater, *Mater. Today Commun.* **2020**, *22*, 100750.
- [129] C. S. Gudipati, J. A. Finlay, J. A. Callow, M. E. Callow, K. L. Wooley, *Langmuir* **2005**, *21*, 3044.
- [130] Y. Wang, D. E. Betts, J. A. Finlay, L. Brewer, M. E. Callow, J. A. Callow, D. E. Wendt, J. M. Desimone, *Macromolecules* **2011**, *44*, 878.
- [131] G. Galli, D. Barsi, E. Martinelli, A. Glisenti, J. A. Finlay, M. E. Callow, J. A. Callow, *RSC Adv.* **2016**, *6*, 67127.
- [132] T. P. Galhenage, D. C. Webster, A. M. S. Moreira, R. J. Burgett, S. J. Stafslien, L. Vanderwal, J. A. Finlay, S. C. Franco, A. S. Clare, *J. Coat. Technol. Res.* **2017**, *14*, 307.
- [133] D. Park, C. J. Weinman, J. A. Finlay, B. R. Fletcher, M. Y. Paik, H. S. Sundaram, M. D. Dimitriou, K. E. Sohn, M. E. Callow, J. A. Callow, D. L. Handlin, C. L. Willis, D. A. Fischer, E. J. Kramer, C. K. Ober, *Langmuir* **2010**, *26*, 9772.
- [134] Y. Cho, H. S. Sundaram, C. J. Weinman, M. Y. Paik, M. D. Dimitriou, J. A. Finlay, M. E. Callow, J. A. Callow, E. J. Kramer, C. K. Ober, *Macromolecules* **2011**, *44*, 4783.
- [135] Y. Cho, H. S. Sundaram, J. A. Finlay, M. D. Dimitriou, M. E. Callow, J. A. Callow, E. J. Kramer, C. K. Ober, *Biomacromolecules* **2012**, *13*, 1864.
- [136] Z. Zhou, D. R. Calabrese, W. Taylor, J. A. Finlay, M. E. Callow, J. A. Callow, D. Fischer, E. J. Kramer, C. K. Ober, *Biofouling* **2014**, *30*, 589.



- [137] M. F. Delcroix, S. Demoustier-Champagne, C. C. Dupont-Gillain, *Langmuir* **2014**, *30*, 268.
- [138] B. M. Wenning, E. Martinelli, S. Mieszkin, J. A. Finlay, D. Fischer, J. A. Callow, M. E. Callow, A. K. Leonardi, C. K. Ober, G. Galli, *ACS Appl. Mater. Interfaces* **2017**, *9*, 16505.
- [139] G. Galli, E. Martinelli, *Macromol. Rapid Commun.* **2017**, *38*, 1600704.
- [140] D. R. Calabrese, B. Wenning, J. A. Finlay, M. E. Callow, J. A. Callow, D. Fischer, C. K. Ober, *Polym. Adv. Technol.* **2015**, *26*, 829.
- [141] W. van Zoelen, R. N. Zuckermann, R. A. Segalman, *Macromolecules* **2012**, *45*, 7072.
- [142] C. Leng, H. G. Buss, R. A. Segalman, Z. Chen, *Langmuir* **2015**, *31*, 9306.
- [143] L. Andersson, L. Blomberg, M. Flegel, L. Lepsa, B. Nilsson, M. Verlander, *Biopolymers* **2000**, *55*, 227.
- [144] A. Isidro-Llobet, M. N. Kenworthy, S. Mukherjee, M. E. Kopach, K. Wegner, F. Gallou, A. G. Smith, F. Roschangar, *J. Org. Chem.* **2019**, *84*, 4615.
- [145] J. A. Callow, M. E. Callow, *Nat. Commun.* **2011**, *2*, 244.
- [146] H. Qi, I. Hölken, A. Gapeeva, V. Filiz, R. Adelung, M. Baum, *Materials* **2018**, *11*, 2413.
- [147] M. S. Selim, S. A. El-Safty, M. A. El-Sockary, A. I. Hashem, O. M. Abo Elenien, A. M. El-Saeed, N. A. Fatthallah, *RSC Adv.* **2015**, *5*, 19933.
- [148] M. S. Selim, S. A. El-Safty, A. M. Azzam, M. A. Shenashen, M. A. El-Sockary, O. M. Abo Elenien, *ChemistrySelect* **2019**, *4*, 3395.
- [149] M. S. Selim, H. Yang, S. A. El-Safty, N. A. Fatthallah, M. A. Shenashen, F. Q. Wang, Y. Huang, *Colloids Surf. A* **2019**, *570*, 518.
- [150] M. S. Selim, H. Yang, F. Q. Wang, N. A. Fatthallah, X. Li, Y. Li, Y. Huang, *J. Coat. Technol. Res.* **2019**, *16*, 1165.
- [151] M. Ba, Y. Wang, X. Yan, *Prog. Org. Coat.* **2019**, *136*, 105266.
- [152] M. Ba, Z. Zhang, Y. Qi, *Prog. Org. Coat.* **2019**, *130*, 132.
- [153] M. Cloutier, D. Mantovani, F. Rosei, *Trends Biotechnol.* **2015**, *33*, 637.
- [154] T. Wei, Z. Tang, Q. Yu, H. Chen, *ACS Appl. Mater. Interfaces* **2017**, *9*, 37511.
- [155] K. Vasilev, *Coatings* **2019**, *9*, 654.
- [156] N. Clarkson, L. V. Evans, *Biofouling* **1995**, *9*, 129.
- [157] E. Oblak, A. Piecuch, A. Krasowska, J. Łuczyński, *Microbiol. Res.* **2013**, *168*, 630.
- [158] J. Hoque, P. Akkapeddi, V. Yadav, G. B. Manjunath, D. S. S. M. Uppu, M. M. Konai, V. Yarlagadda, K. Sanyal, J. Haldar, *ACS Appl. Mater. Interfaces* **2015**, *7*, 1804.
- [159] L. Liu, H. Shi, H. Yu, R. Zhou, J. Yin, S. Luan, *Biomater. Sci.* **2019**, *7*, 5035.
- [160] J. Zhao, L. Ma, W. Millians, T. Wu, W. Ming, *ACS Appl. Mater. Interfaces* **2016**, *8*, 8737.
- [161] W. Yang, F. Zhou, *Biosurf. Biotribol.* **2017**, *3*, 97.
- [162] Y. J. Oh, E. S. Khan, A. Del Campo, P. Hinterdorfer, B. Li, *ACS Appl. Mater. Interfaces* **2019**, *11*, 29312.
- [163] S. B. Lee, R. R. Koepsel, S. W. Morley, K. Matyjaszewski, Y. Sun, A. J. Russell, *Biomacromolecules* **2004**, *5*, 877.
- [164] L. A. T. W. Asri, M. Crismaru, S. Roest, Y. Chen, O. Ivashenko, P. Rudolf, J. C. Tiller, H. C. van der Mei, T. J. A. Loontjens, H. J. Busscher, *Adv. Funct. Mater.* **2014**, *24*, 346.
- [165] S. Roest, H. C. van der Mei, T. J. A. Loontjens, H. J. Busscher, *Appl. Surf. Sci.* **2015**, *356*, 325.
- [166] J. J. Dong, A. Muszanska, F. Xiang, R. Falkenberg, B. van de Belt-Gritter, T. Loontjens, *Langmuir* **2019**, *35*, 14108.
- [167] P. Zhao, F. Mecozi, S. Wessel, B. Fieten, M. Driese, W. Woudstra, H. J. Busscher, H. C. van der Mei, T. J. A. Loontjens, *Langmuir* **2019**, *35*, 5779.
- [168] J. Yue, P. Zhao, J. Y. Gerasimov, M. van de Lagemaat, A. Grotenhuis, M. Rustema-Abbing, H. C. van der Mei, H. J. Busscher, A. Herrmann, Y. Ren, *Adv. Funct. Mater.* **2015**, *25*, 6756.
- [169] Q. Yu, J. Cho, P. Shivapooja, L. K. Ista, G. P. López, *ACS Appl. Mater. Interfaces* **2013**, *5*, 9295.
- [170] K. Herget, P. Hubach, S. Pusch, P. Deglmann, H. Götz, T. E. Gorelik, I. A. Gural'skiy, F. Pfitzner, T. Link, S. Schenk, M. Panthöfer, V. Ksenofontov, U. Kolb, T. Opatz, R. André, W. Tremel, *Adv. Mater.* **2017**, *29*, 1603823.
- [171] M. Hu, K. Korschelt, M. Viel, N. Wiesmann, M. Kappl, J. Brieger, K. Landfester, H. Thérien-Aubin, W. Tremel, *ACS Appl. Mater. Interfaces* **2018**, *10*, 44722.
- [172] L. Chen, Y. Yang, P. Zhang, S. Wang, J. F. Xu, X. Zhang, *ACS Appl. Bio Mater.* **2019**, *2*, 2920.
- [173] W. Sim, R. T. Barnard, M. A. T. Blaskovich, Z. M. Ziora, *Antibiotics* **2018**, *7*, 93.
- [174] S. Nakamura, M. Sato, Y. Sato, N. Ando, T. Takayama, M. Fujita, M. Ishihara, *Int. J. Mol. Sci.* **2019**, *20*, 3620.
- [175] K. Vasilev, V. Sah, K. Anselme, C. Ndi, M. Mateescu, B. Dollmann, P. Martinek, H. Ys, L. Ploux, H. J. Griesser, *Nano Lett.* **2010**, *10*, 202.
- [176] F. Paladini, M. Pollini, *Materials* **2019**, *12*, 2540.
- [177] W. L. Olinari, D. F. Parra, L. F. C. P. Lima, N. Lincopan, A. B. Lugao, *J. Appl. Polym. Sci.* **2015**, *132*, 42218.
- [178] G. Cao, H. Lin, P. Kannan, C. Wang, Y. Zhong, Y. Huang, Z. Guo, *Langmuir* **2018**, *34*, 14537.
- [179] D. Tomacheski, M. Pittol, V. Ferreira Ribeiro, R. Marlene Campomanes Santana, *J. Appl. Polym. Sci.* **2016**, *133*, 1.
- [180] D. Mitra, E. T. Kang, K. G. Neoh, *ACS Appl. Mater. Interfaces* **2020**, <https://doi.org/10.1021/acsami.9b17815>.
- [181] D. A. Montero, C. Arellano, M. Pardo, R. Vera, R. Gálvez, M. Cifuentes, M. A. Berasain, M. Gómez, C. Ramírez, R. M. Vidal, *Antimicrob. Resist. Infect. Control* **2019**, *8*, 3.
- [182] D. Mitra, M. Li, E. T. Kang, K. G. Neoh, *ACS Appl. Mater. Interfaces* **2019**, *11*, 73.
- [183] O. Bondarenko, K. Juganson, A. Ivask, K. Kasemets, M. Mortimer, A. Kahru, *Arch. Toxicol.* **2013**, *87*, 1181.
- [184] S. M. Olsen, L. T. Pedersen, M. H. Laursen, S. Kiil, K. Dam-Johansen, *Biofouling* **2007**, *23*, 369.
- [185] D. Alves, M. Olívia Pereira, *Biofouling* **2014**, *30*, 483.
- [186] J. B. Kristensen, R. L. Meyer, B. S. Laursen, S. Shipovskov, F. Besenbacher, C. H. Poulsen, *Biotechnol. Adv.* **2008**, *26*, 471.
- [187] E. Aykin, B. Omuzbukun, A. Kacar, *J. Coat. Technol. Res.* **2019**, *16*, 847.
- [188] C. Wu, K. Schwibbert, K. Achazi, P. Landsberger, A. Gorbushina, R. Haag, *Biomacromolecules* **2017**, *18*, 210.
- [189] J. A. Park, S. C. Lee, S. B. Kim, *J. Mater. Sci.* **2019**, *54*, 9969.
- [190] K. M. Yeon, J. You, M. D. Adhikari, S. G. Hong, I. Lee, H. S. Kim, L. N. Kim, J. Nam, S. J. Kwon, M. Il Kim, W. Sajomsang, J. S. Dordick, J. Kim, *Biomacromolecules* **2019**, *20*, 2477.
- [191] K. Herget, H. Frerichs, F. Pfitzner, M. N. Tahir, W. Tremel, *Adv. Mater.* **2018**, *30*, 1707073.
- [192] J. Wu, X. Wang, Q. Wang, Z. Lou, S. Li, Y. Zhu, L. Qin, H. Wei, *Chem. Soc. Rev.* **2019**, *48*, 1004.
- [193] Z. Liu, F. Wang, J. Ren, X. Qu, *Biomaterials* **2019**, *208*, 21.
- [194] M. Q. Mesquita, C. J. Dias, M. G. P. M. S. Neves, A. Almeida, M. A. F. Faustino, *Molecules* **2018**, *23*, 2424.
- [195] K. Liu, M. Cao, A. Fujishima, L. Jiang, *Chem. Rev.* **2014**, *114*, 10044.
- [196] X. Wei, Z. Yang, S. L. Tay, W. Gao, *Appl. Surf. Sci.* **2014**, *290*, 274.
- [197] C. Chambers, S. B. Stewart, B. Su, H. F. Jenkinson, J. R. Sandy, A. J. Ireland, *Dent. Mater.* **2017**, *33*, e115.
- [198] Z. Xu, T. Wu, J. Shi, K. Teng, W. Wang, M. Ma, J. Li, X. Qian, C. Li, J. Fan, *J. Membr. Sci.* **2016**, *520*, 281.
- [199] M. A. Fitri, M. Ota, Y. Hirota, Y. Uchida, K. Hara, D. Ino, N. Nishiyama, *Mater. Chem. Phys.* **2017**, *198*, 42.
- [200] M. T. Taghizadeh, V. Siyahi, H. Ashassi-Sorkhabi, G. Zarrini, *Int. J. Biol. Macromol.* **2020**, *147*, 1018.
- [201] N. Mohri, H. Kerschbaumer, T. Link, R. Andre, M. Panthöfer, V. Ksenofontov, W. Tremel, *Eur. J. Inorg. Chem.* **2019**, *2019*, 3171.

- [202] A. Joshi, S. Punyani, S. S. Bale, H. Yang, T. Borca-Tasciuc, R. S. Kane, *Nat. Nanotechnol.* **2008**, *3*, 41.
- [203] N. Tsolekile, S. Nelana, O. S. Oluwafemi, *Molecules* **2019**, *24*, 2669.
- [204] D. A. Heredia, S. R. Martínez, A. M. Durantini, M. E. Pérez, M. I. Mangione, J. E. Durantini, M. A. Gervaldo, L. A. Otero, E. N. Durantini, *ACS Appl. Mater. Interfaces* **2019**, *11*, 27574.
- [205] Q. Pan, S. Zhang, R. Li, Y. He, Y. Wang, *J. Mater. Chem. B* **2019**, *7*, 2948.
- [206] P. Shivapooja, Q. Yu, B. Orihuela, R. Mays, D. Rittschof, J. Genzer, G. P. López, *ACS Appl. Mater. Interfaces* **2015**, *7*, 25586.
- [207] Q. Gao, M. Yu, Y. Su, M. Xie, X. Zhao, P. Li, P. X. Ma, *Acta Biomater.* **2017**, *51*, 112.
- [208] X. Wang, S. Yan, L. Song, H. Shi, H. Yang, S. Luan, Y. Huang, J. Yin, A. F. Khan, J. Zhao, *ACS Appl. Mater. Interfaces* **2017**, *9*, 40930.
- [209] B. Xu, Y. Liu, X. Sun, J. Hu, P. Shi, X. Huang, *ACS Appl. Mater. Interfaces* **2017**, *9*, 16517.
- [210] A. Kirillova, C. Marschelke, J. Friedrichs, C. Werner, A. Synytska, *ACS Appl. Mater. Interfaces* **2016**, *8*, 32591.
- [211] Y. Wang, Z. Wang, J. Wang, S. Wang, *J. Membr. Sci.* **2018**, *549*, 495.
- [212] T. Wei, W. Zhan, Q. Yu, H. Chen, *ACS Appl. Mater. Interfaces* **2017**, *9*, 25767.
- [213] B. Xu, C. Feng, J. Hu, P. Shi, G. Gu, L. Wang, X. Huang, *ACS Appl. Mater. Interfaces* **2016**, *8*, 6685.
- [214] J. Yang, H. Chen, S. Xiao, M. Shen, F. Chen, P. Fan, M. Zhong, J. Zheng, *Langmuir* **2015**, *31*, 9125.
- [215] D. L. Huber, R. P. Manginell, M. A. Samara, B.-I. Kim, B. C. Bunker, *Science* **2003**, *301*, 352.
- [216] M. Divandari, J. Pollard, E. Dehghani, N. Bruns, E. M. Benetti, *Biomacromolecules* **2017**, *18*, 4261.
- [217] J. Zheng, B. D. Vogt, R. Hu, M. Zhang, L. Li, S. Xiao, S. M. Bhaway, Y. Chang, Q. Chen, J. Ma, J. Yang, H. Chen, *Acta Biomater.* **2016**, *40*, 62.
- [218] D. Zhang, Y. Fu, L. Huang, Y. Zhang, B. Ren, M. Zhong, J. Yang, J. Zheng, *J. Mater. Chem. B* **2018**, *6*, 950.
- [219] K. H. Chae, Y. M. Jang, Y. H. Kim, O. J. Sohn, J. Il Rhee, *Sens. Actuators, B* **2007**, *124*, 153.
- [220] A. Gapeeva, I. Hölken, R. Adelung, M. Baum, *Proc. of the 2017 IEEE 7th Int. Conf. on Nanomaterials: Applications and Properties (NAP)*, IEEE, Piscataway, NJ **2017**, pp. 1–5.
- [221] W. Wang, R. A. Siegel, C. Wang, *ACS Biomater. Sci. Eng.* **2016**, *2*, 180.
- [222] D. Chen, M. Wu, B. Li, K. Ren, Z. Cheng, J. Ji, Y. Li, J. Sun, *Adv. Mater.* **2015**, *27*, 5882.
- [223] B. V. S. Iyer, V. V. Yashin, A. C. Balazs, *Polymer* **2015**, *69*, 310.
- [224] Z. Wang, H. Zuilhof, *J. Mater. Chem. A* **2016**, *4*, 2408.
- [225] Z. Wang, H. Zuilhof, *Langmuir* **2016**, *32*, 6310.
- [226] Z. Wang, E. van Andel, S. P. Pujari, H. Feng, J. A. Dijkman, M. M. J. Smulders, H. Zuilhof, *J. Mater. Chem. B* **2018**, *6*, 6930.
- [227] Z. Wang, G. Fei, H. Xia, H. Zuilhof, *J. Mater. Chem. B* **2017**, *5*, 6728.
- [228] B. L. Mbang, B. V. S. Iyer, V. V. Yashin, A. C. Balazs, *Macromolecules* **2016**, *49*, 1353.
- [229] K. C. Dansuk, S. Keten, *Matter* **2019**, *1*, 911.
- [230] E. Spruijt, *PhD Thesis*, Wageningen University, **2012**.
- [231] W. M. De Vos, J. M. Kleijn, M. A. C. Stuart, *Polymer Brushes: Substrates, Technologies, and Properties*, CRC Press, London **2012**, pp. 133–162.
- [232] W. M. De Vos, J. M. Kleijn, A. De Keizer, M. A. C. Stuart, *Angew. Chem., Int. Ed.* **2009**, *48*, 5369.
- [233] X. Zhu, D. Jańczewski, S. Guo, S. S. C. Lee, F. J. Parra Velandia, S. L. M. Teo, T. He, S. R. Puniredd, G. Julius Vancso, *ACS Appl. Mater. Interfaces* **2015**, *7*, 852.
- [234] C. Cortez, J. F. Quinn, X. Hao, C. S. Gudipati, M. H. Stenzel, T. P. Davis, F. Caruso, *Langmuir* **2010**, *26*, 9720.
- [235] L. Yu, Y. Hou, C. Cheng, C. Schlaich, P. L. M. Noeske, Q. Wei, R. Haag, *ACS Appl. Mater. Interfaces* **2017**, *9*, 44281.
- [236] H. S. Sundaram, X. Han, A. K. Nowinski, N. D. Brault, Y. Li, J. R. Ella-Menye, K. A. Amoaka, K. E. Cook, P. Marek, K. Senecal, S. Jiang, *Adv. Mater. Interfaces* **2014**, *1*, 1400071.
- [237] Z. H. Wu, H. B. Chen, Y. M. Dong, H. L. Mao, J. L. Sun, S. F. Chen, V. S. J. Craig, J. Hu, *J. Colloid Interface Sci.* **2008**, *328*, 10.
- [238] Z. Cao, T. Gan, G. Xu, C. Ma, *Langmuir* **2019**, *35*, 14596.
- [239] W. M. de Vos, A. de Keizer, M. A. C. Stuart, J. M. Kleijn, *Colloids Surf. A* **2010**, *358*, 6.
- [240] H. Chen, H. Mao, L. Wu, J. Zhang, Y. Dong, Z. Wu, J. Hu, *Biofouling* **2009**, *25*, 353.
- [241] W. Gao, H. Liang, J. Ma, M. Han, Z. Chen, Z. Han, G. Li, *Desalination* **2011**, *272*, 1.
- [242] A. L. Lim, R. Bai, *J. Membr. Sci.* **2003**, *216*, 279.
- [243] M. Okochi, H. Yokokawa, T. K. Lim, T. Taguchi, H. Takahashi, H. Yokouchi, T. Kaiho, A. Sakuma, T. Matsunaga, *Appl. Environ. Microbiol.* **2005**, *71*, 6410.
- [244] M. Muthu, J. Gopal, S. Chun, S. K. Lee, *Arabian J. Sci. Eng.* **2018**, *43*, 241.
- [245] L. Piculell, J. Sjöström, I. Lynch, *Aqueous Polymer — Cosolute Systems. Progress in Colloid and Polymer Science* (Ed: D. F. Anghel), Vol. 122, Springer, Berlin.
- [246] Q. Xie, X. Zhou, C. Ma, G. Zhang, *Ind. Eng. Chem. Res.* **2017**, *56*, 5318.
- [247] S. Ilyas, J. de Groot, K. Nijmeijer, W. M. De Vos, *J. Colloid Interface Sci.* **2015**, *446*, 386.
- [248] S. Cao, J. D. Wang, H. S. Chen, D. R. Chen, *Chin. Sci. Bull.* **2011**, *56*, 598.